REPORT DOCUMENTATION PAGE

AFRL-SR-BL-TR-98

0597

1. AGENCY USE ONLY *(Leave blank)*	2. REPORT DATE	3. REPORT TYPE AND DATES COVERED
	August 1998	FINAL REPORT 1 Jul 95 - 14 May 98

4. TITLE AND SUBTITLE
MECHANICAL/THERMAL JET SURFACE INTERACTIONS IN PAINT STRIPPING PROCESSES

5. FUNDING NUMBERS
F49620-95-C-0048

61102F
2307/BS

6. AUTHOR(S)
D. PAREKH, A. GLEZER, T. CRITTENDEN, C. ROGERS, L. MEADE, S. POTHIER, J. KELLEY, AND Y. IKEDA

7. PERFORMING ORGANIZATION NAME(S) AND ADDRESS(ES)
BOEING COMPANY
PO BOX 516
ST LOUIS MO 63166-0516

8. PERFORMING ORGANIZATION REPORT NUMBER

9. SPONSORING/MONITORING AGENCY NAME(S) AND ADDRESS(ES)
AIR FORCE OFFICE OF SCIENTIFIC RESEARCH (AFOSR)
110 DUNCAN AVENUE ROOM B115
BOLLING AFB DC 20332-8050

10. SPONSORING/MONITORING AGENCY REPORT NUMBER

11. SUPPLEMENTARY NOTES

12a. DISTRIBUTION AVAILABILITY STATEMENT
APPROVED FOR PUBLIC RELEASE, DISTRIBUTION IS UNLIMITED

12b. DISTRIBUTION CODE

13. ABSTRACT *(Maximum 200 words)*

Several key accomplishments of this program are highlighted below: Experimental results for the two-phase flow were obtained on a full-scale production paint stripping system since this was the best way to assure that the relevant flow and system parameters were being considered. 1. Several key characteristics of two-phase nozzle flow have been characterized, including CO2 pellet sizing, distribution, velocity, sublimation and breakup. Initial results from a statistical analysis of this data is presented in the paper by Meade et al. (1997). The pellet breakup within the delivery system results in a reduction in the pellet size and an increase in number density. 2. Detailed flow visualization and surface static pressure distributions within a very high aspect ratio rectangular jet have been acquired. Pressure distributions were mapped both with and without CO2 pellets. Sublimation of the pellets within the delivery system results in the nozzle operating at a higher pressure ratio than the baseline air only case. Gaseous CO2 concentration levels were characterized at the nozzle exit. 3. Navier-Stokes simulations of internal nozzle flow were completed and estimates of particle trajectories were obtained by post-processing the steady-state flow solutions, using an analytical model for the particle drag. 4. Supporting diagnostic efforts led to the development of a new two-camera PIV technique and initial application to two-phase jet flow (Pothier et al., 1997). 5. To provide a suitable actuator for control of this class of particle laden flows, development of a novel piston-cylinder synthetic jet actuator capable of producing supersonic peak velocities was initiated. An isentropic model to predict the time-dependent pressure in the cylinder for use in optimizing the actuator design was formalized and validated.

14. SUBJECT TERMS

19980903 001

15. NUMBER OF PAGES
48

16. PRICE CODE

17. SECURITY CLASSIFICATION OF REPORT	18. SECURITY CLASSIFICATION OF THIS PAGE	19. SECURITY CLASSIFICATION OF ABSTRACT	20. LIMITATION OF ABSTRACT
UNCLASSIFIED	UNCLASSIFIED	UNCLASSIFIED	

Characterization of Particle-Laden Nozzle Flows Associated with Paint-Stripping Processes

D. E. Parekh, A. Glezer, and T. Crittenden
Georgia Institute of Technology, Atlanta, GA 30332

C. B. Rogers, L. Meade, and S. Pothier
Tufts University, Medford, MA 02155

J. D. Kelley and Y. Ikeda
Boeing Company, St. Louis, MO 63166

14 August 1998
Final Technical Report
Contract F49620-95-C-0048

Prepared for:
Dr. Mark Glauser and Dr. James McMichael
UNITED STATES AIR FORCE
Air Force Office of Scientific Research
Bolling Air Force Base, DC 20332

The Boeing Company
P.O. Box 516
St. Louis, MO 63166-0516
(314) 232-0232 TELEX 44-857

AFOSR-018-40132

14 August 1998

Subject: Contract F49620-95-C-0048; "Mechanical /Thermal Jet-Surface Interactions in Paint Stripping Processes"; Submittal of Final Report

To: AFOSR/NA
Directorate of Aerospace and Materials Sciences
110 Duncan Ave., Suite B115
Bolling AFB
Washington, DC 20084-8080

Attention: Dr. Mark Glauser

Enclosure: (1) Final Technical Report ; Characterization and Control of Two-Phase Impinging Jets in Paint Stripping Processes (3 Copies)

1. McDonnell Douglas Corporation (MDC), a wholly owned subsidiary of The Boeing Company, in accordance with the subject contract, is hereby pleased to submit Enclosure (1) as our final technical report for the subject program, in accordance with CLIN 0002AA of the subject contract. MDC will submit a formal DD Form 250 for AFOSR's execution under separate cover.

2. Should you have any questions, please feel free to contact the undersigned at (314) 233-7911.

W. H. Cole

W. H. Cole
Specialist - Contracts and Pricing
Phantom Works (WHC Disk –0048)

EC: AFOSR/PKA (Ltr. Only)
110 Duncan Ave., Suite B115
Bolling Air Force Base
Washington, DC 20332-8080
Attn.: Jennifer Bell , Contract Administrator

AFOSR/PKA (Ltr. Only)
110 Duncan Ave., Suite B115
Bolling Air Force Base
Washington, DC 20332-8080
Attn.: Ms. Gerri Wilson

DCMC S3061375 (Ltr. Only)

ENCLOSURE (1)

TO

AFOSR-018-40132

CLIN 0002AA - FINAL TECHNICAL REPORT
CHARACTERIZATION AND CONTROL OF TWO-PHASE IMPINGING JETS
IN PAINT STRIPPING PROCESSES (3 COPIES)

EXECUTIVE SUMMARY

Objective. The primary objective of this study is to gain fundamental understanding of the physical mechanisms associated with impinging particle-laden jet flows typical of paint stripping processes. Special emphasis is given to high-aspect-ratio jets and to high speed air flows seeded with solid CO2 pellets. These basic research investigations are focused to yield new concepts and system level improvements for a variety of coatings removal and surface preparation applications.

Accomplishments. Several key accomplishments of this program are highlighted below: Experimental results for the two-phase flow were obtained on a full-scale production paint stripping system since this was the best way to assure that the relevant flow and system parameters were being considered.

1) Several key characteristics of two-phase nozzle flow have been characterized, including CO2 pellet sizing, distribution, velocity, sublimation and breakup. Initial results from a statistical analysis of this data is presented in the paper by Meade et al. (1997). The pellet breakup within the delivery system results in a reduction in the pellet size and an increase in number density.

2) Detailed flow visualization and surface static pressure distributions within a very high aspect ratio rectangular jet have been acquired. Pressure distributions were mapped both with and without CO2 pellets. Sublimation of the pellets within the delivery system results in the nozzle operating at a higher pressure ratio than the baseline air only case. Gaseous CO2 concentration levels were characterized at the nozzle exit.

3) Navier-Stokes simulations of internal nozzle flow were completed and estimates of particle trajectories were obtained by post-processing the steady-state flow solutions, using an analytical model for the particle drag.

4) Supporting diagnostic efforts led to the development of a new two-camera PIV technique and initial application to two-phase jet flow (Pothier et al., 1997).

5) To provide a suitable actuator for control of this class of particle-laden flows, development of a novel piston-cylinder synthetic jet actuator capable of producing supersonic peak velocities was initiated. An isentropic model to predict the time-dependent pressure in the cylinder for use in optimizing the actuator design was formalized and validated.

This report provides a detailed description of the technical approach and results associated with the first two accomplishments. This represents the major portion of the research endeavor. The three other accomplishments have been or will be documented through archived technical papers.

References

1. L. Meade, S. Pothier, C. Rogers, and D. Parekh, An Investigation of Particle Behavior in a Compressible, Impinging Jet Flow. AIAA paper 97-1994. AIAA Fluid Dynamics Conference, Snowmass Village, CO, 1997.

2. S. Pothier, J. Bellerose, C. Rogers, and D. Parekh, Analysis of Small High Speed CO_2 Particles Using Low-Cost Video Imaging Systems, AIAA paper 97-0856. AIAA Aerospace Sciences Meeting, Reno, NV, 1997.

1. INTRODUCTION

The use of particle-laden impinging jet flows is common to several paint stripping techniques. To maximize stripping width and minimize particle use, these techniques typically employ very high-aspect-ratio nozzles. The objective of this work is to characterize the particle behavior within these types of nozzles to provide the fundamental understanding needed to optimize nozzle designs for enhanced performance and reduced operating costs. Several people have looked at particle velocities in nozzles[1] and have even examined particle trajectories in two-phase flow systems[2], but this work has been done at slower flow speeds than those considered here. Others[3,4,5] have tried to determine accurate drag coefficients for gas-particle flows. No previous research has been foundon particle behavior for compressible flow through a nozzle.

The FLASHJET® coatings removal process is one example of a paint removal technique that uses CO_2 pellet flow. The process is an environmentally friendly, cost effective, safe way to remove surface coatings. It is equally effective on metals and composites. The system uses a combination of high energy pulsed light, a low pressure solid CO_2 particle stream, an effluent capture vacuum system, and a process control system (Figure 1). A ColdJet Inc. pelletizer, which is part of the FLASHJET® system, uses a high pressure hydraulic cylinder and piston assembly to form CO_2 pellets from liquid CO_2. These pellets are combined with a compressed air stream and sent through a long flexible hose, typically longer than 30 m, to the delivery nozzle which is mounted on the stripping head. As the pellets are accelerated through the hose they are broken up and partially sublime. The resulting particle/gas flow exits through a high-aspect-ratio, converging-diverging nozzle. The stripping head, which also holds the flashlamp and vacuum system, is mounted on a 7-axis gantry robot which is used to move the stripping head over a pre-

programmed path in order to strip airplane components. A flashlamp emits pulsed light energy which pyrolizes the paint layer, and the high speed particle impingement removes the surface residue and helps cool the substrate. All residue is captured by the vacuum system Figure 2 shows the FLASHJET® in action and the difference between the painted surface and the surface being cleaned is clearly visible.

From an operational standpoint, the goal of this work is understand what is happening with the particles so that we can come up with a design for a more compact nozzle, reduce the amount of CO_2 that is used, and minimize the pressure that is necessary to run the system without compromising its effectiveness in stripping paint. A compact nozzle will allow for easier manuevering around difficult objects. The greatest operating cost item is the liquid CO_2, and one of the largest startup costs is the air compressor. Gaining a better understanding of the particle behavior both on the surface and inside the nozzle will help to optimize the nozzle and thus reduce operating costs. From a research standpoint, the goal is to gain a better understanding of the particle behavior inside the nozzle.

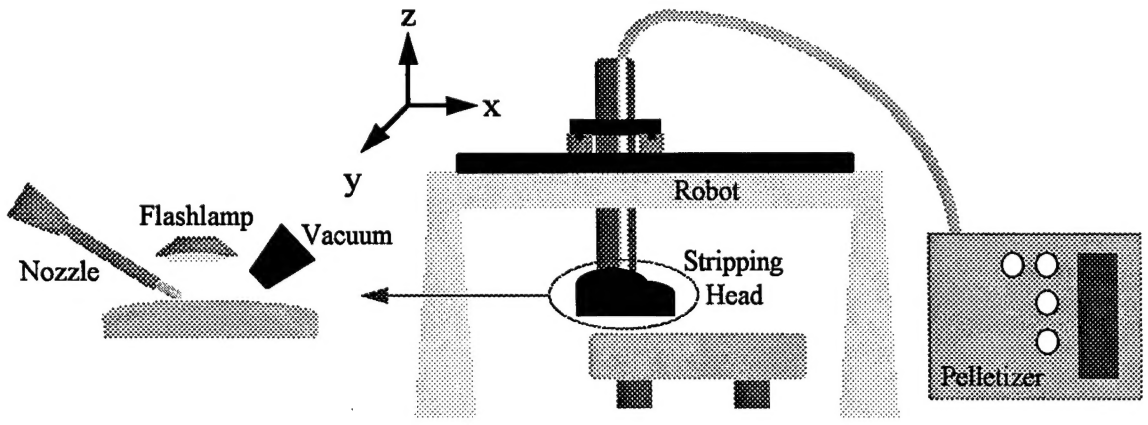

Figure 1 - Schematic of FLASHJET® System

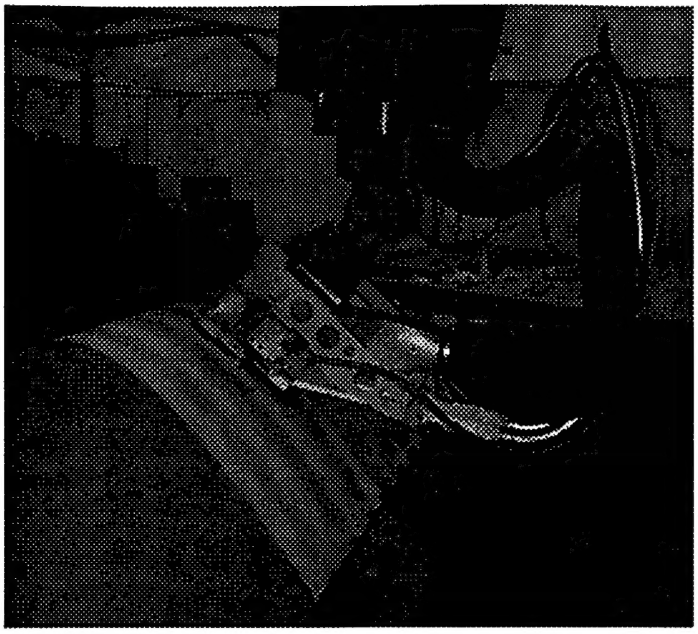

Figure 2 - FLASHJET® in Action

2. EXPERIMENTAL SETUP AND PROCEDURE

The greatest challenge in this investigation was taking measurements on a production FLASHJET® system. To produce the relevant operating conditions, it was found necessary to use a production rather than a laboratory apparatus, but this limited our choice in diagnostic techniques and reduced the testing flexibility. To make measurements on a production system, we chose four different methods to characterize flow and particle behavior: 1) static and stagnation pressure measurements inside the nozzle and at the exit, 2) laser Doppler velocimeter measurements in the entrance of the nozzle, 3) image processing for estimating particle diameters through the nozzle and particle concentration at the exit, and 4) flow visualization for examining flow patterns in the nozzle.

We could not use a number of anemometry techniques due to limitations of taking data on the working system. Laser Doppler Anemometry measurements at the exit could not be taken because it would have been necessary to use a high powered laser which was not allowed on the manufacturing floor. Hotwire measurements were not an option because the particles in the flow would have broken the wires. Particle Image Velocimetry was not a possibilty due to a lack of enough pulsed energy, which could only come from a pulsed YAG laser. The temperature of the the CO_2 flow was too low to use an infrared camera images to learn more about the heat transfer of the particles on the surface being cleaned.

2.1 NOZZLES

The FLASHJET® nozzle is a high-aspect-ratio, converging-diverging nozzle with an overall length of 49.5 cm, a width of 33 cm, and an exit height of 0.16 cm. Figure 3 shows the

standard FLASHJET® nozzle which converges vertically to a minimum throat section of 2.9 cm x 0.16 cm, and expands horizontally in the supersonic divergent section. The expansion section is of constant height which is equal to the exit height and has a length of 39.4 cm. Two prototype nozzles were built and used to acquire all measurements. One was constructed with Plexiglas so that the flow could be seen inside the nozzle. The other was made with metal so that pressure taps could be easily mounted on this nozzle. Using metal to build this nozzle also ensures that the temperature of the flow is the same as the temperature of the flow through the standard FLASHJET® nozzle. Figure 4 shows the transparent Plexiglass nozzle which was used to obtain the laser Doppler velocimeter measurements, image processing data, flow visualization images, and stagnation pressure measurements. This nozzle is similar to one-half of the standard nozzle except that its expansion length and width are about 9% less. These are the dimensions of the original FLASHJET® nozzle. Its entrance and contraction section are the same height and length as the standard nozzle. The final nozzle, seen in Figure 5, was used to take static pressure measurements. It is a metal nozzle, with the same dimensions as the transparent nozzle, that was modified with twenty static pressure taps along its centerline and in the spanwise direction at x/h of 216 and 283. The transparent nozzle and the metal nozzle mounted with static pressure taps are of equal size and these two nozzles are slightly smaller than the nozzle on the working setup. The nozzles were connected to the long flexible hose which delivers the pellet/air flow from the pelletizer. This ensured that the flow field observed in the test nozzles was similar to the standard FLASHJET® nozzle .

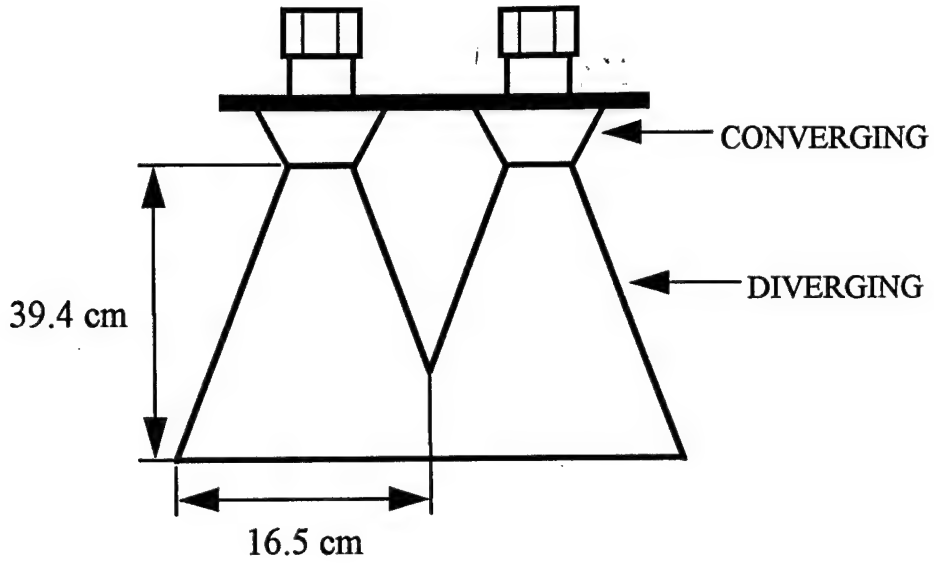

Figure 3 - Standard FLASHJET® Nozzle

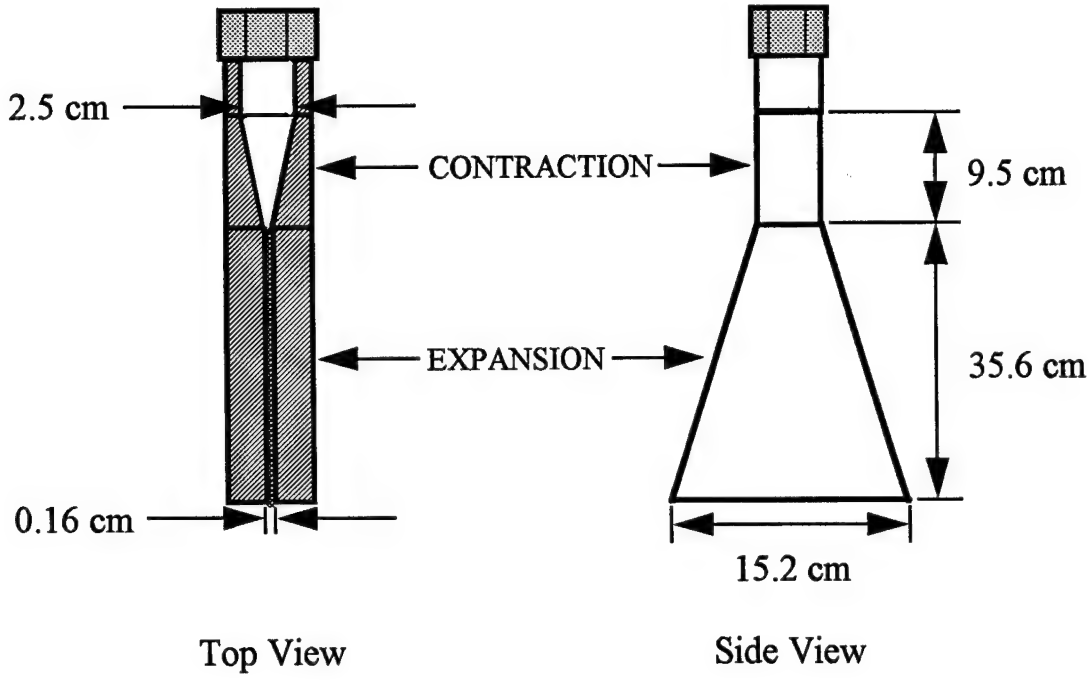

Figure 4 - Transparent Nozzle

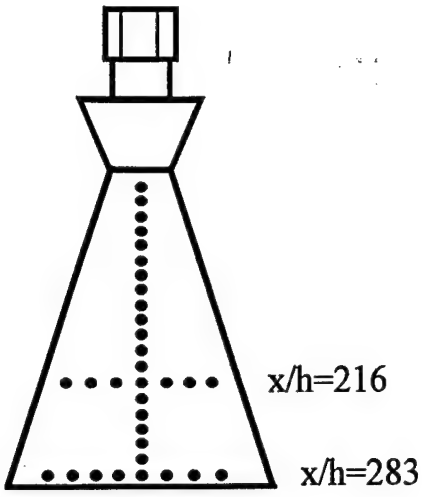

Figure 5 - Nozzle Mounted with Static Pressure Taps

2.2 PRESSURE MEASUREMENTS

The nozzle mounted with pressure taps was used to take static pressure measurements along the centerline of the nozzle and in two spanwise directions at x/h of 216 and 283 (Figure 6). A single 50-psid Druck pressure transducer with a sensitivity of 1.5 mv/psid was used to take the static pressure measurements. Connections to the individual taps was manually cycled to scan all the desired static pressures. The transducer was connected to an A/D board which was run by a Machintosh Powerbook using LabVIEW drivers. At each tap, 1000 samples were taken at a sample rate of 100 Hz. The system can be run with only air through the nozzle or by turning on the pellet flow and accelerating the CO_2 particles through the nozzle. Readings were taken for both cases. The pressure at the pelletizer was set at the normal running pressure of 1100 kPa for these runs. Six centerline and four spanwise runs were taken over two days at different times

during the day and with different levels of frost build-up on the nozzle due to the extreme cold when the pellet flow is on. Both the centerline and spanwise runs showed excellent repeatability and the uncertainties are presented in the results section. Finally, temporal variations were characterized by interrogating a single tap over a five minute period. The results of this showed a fluctuation in the pressure. This led to taking centerline measurements relative to the first tap so that any fluctuations that occur over the course of a run would be factored out. One run was also taken with matching back pressures in the nozzle for the pellets off and on cases.

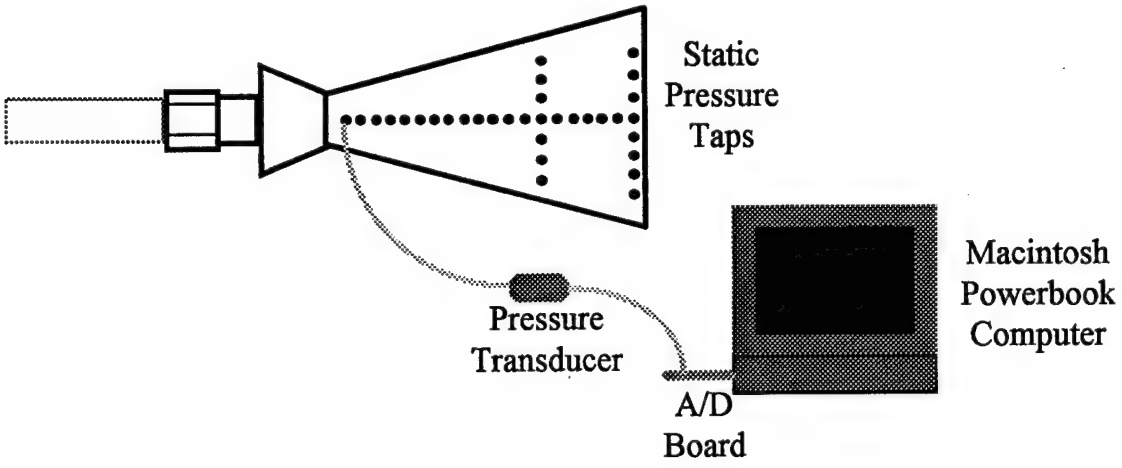

Figure 6 - Static Pressure Measurement Setup

Centerline and spanwise stagnation pressure measurements were taken on the transparent nozzle. The nozzle was mounted on a 2-D traverse and was moved relative to the stationary probe (Figure 7). A pitot probe with a 50 psid Druck pressure transducer with a sensitivity of 1.5 mv/psid was connected to a Fluke digital multimeter. Measurements were taken with both the pellet flow off and on at a pelletizer pressure of 1100 kPa. Centerline measurements were taken every 0.3175 cm for the first 5 cm and then at every 0.635 cm for the pellets off case. For the pellets on case, centerline measurements were only taken every 0.635 cm. Spanwise pressure profiles were taken at x=2h, where x is the streamwise direction beyond the nozzle exit and h is

the nozzle exit height. Spanwise measurements were taken every 0.635 cm along the exit for both the case of pellets off and the case of pellets on. The pressures were calculated by averaging the transducer readings over 10 seconds. Pellets-on measurements have a larger uncertainty and fewer data points due to the low temperature causing the pitot probe to freeze up.

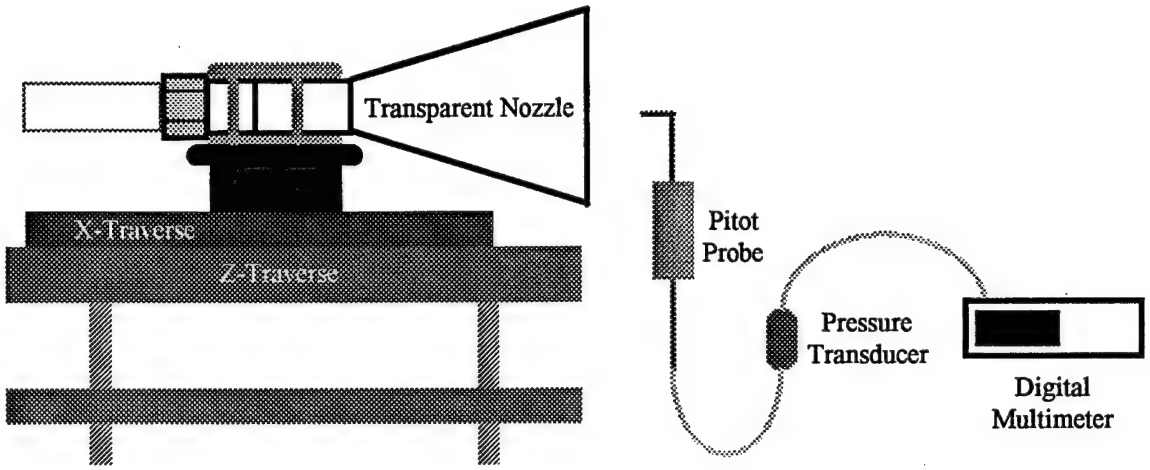

Figure 7 - Stagnation Pressure Measurement Setup

2.3 LASER DOPPLER ANEMOMETRY

Pellet velocities entering the nozzle were obtained using a one-component forward scatter LDA setup. A 5 milliwattt Helium-Neon laser beam was sent through a beam splitter and the measuring volume was aligned along the centerline inside the entrance section of the transparent nozzle (Figure 8). The reflected light was detected by the collecting optics and the frequency shifts were read by an IFA 550 which was controlled by a Macintosh Power PC using LabVIEW drivers. The nozzle was mounted on a 1-D traverse and was moved in the x direction. Velocities were recorded beginning in the entrance section at x/h=6 and ending at x/h=54 which is located just inside the contraction section. The standard deviation across all measurements is less than 1 m/s.

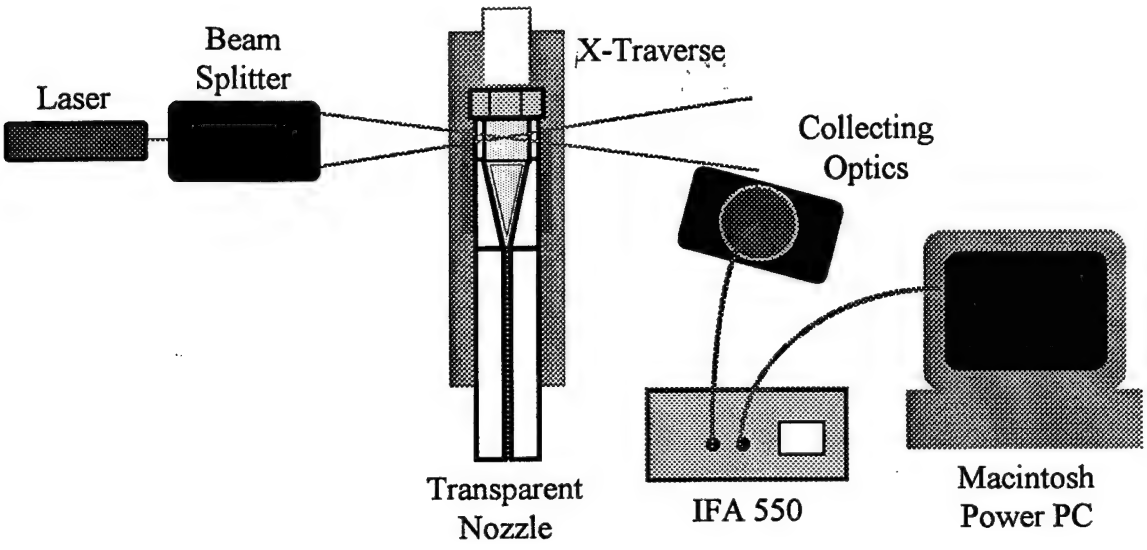

Figure 8 - LDA Setup

Several problems arose in making LDA measurements. First, due to hardware limitations, the LDA system could only measure velocities below 45 m/s. Higher velocities required a higher power laser which was not allowed in the production facility. Second, the particle concentration was too large in the thin parts of the nozzle for accurate readings. Too many particles in the measuring volume reduced the data rate because the system cannot distinguish between the numerous particles that are passing through the fringes.

2.4 IMAGE PROCESSING

The most effective measurement method was using imaging techniques to estimate particle diameter, concentration, and velocity, as well as to gain some physical insight into the particle and flow behavior. A Cohu CCD camera was mounted on a 1-D traverse eqiupped with a position controller. The camera was focused on a ruler along the centerline of the transparent nozzle at several locations inside the nozzle and at the exit. The known distance of the ruler was used to

determine the diameter of the particles. The particles were forzen with a strobe light and images were recorded to an SVHS video recorder (Figure 9). By examining images, we see that the particles are further broken up as they travel through the nozzle. By interrogating the images, we were able to estimate the size of the particles throughout the nozzle and at the exit.

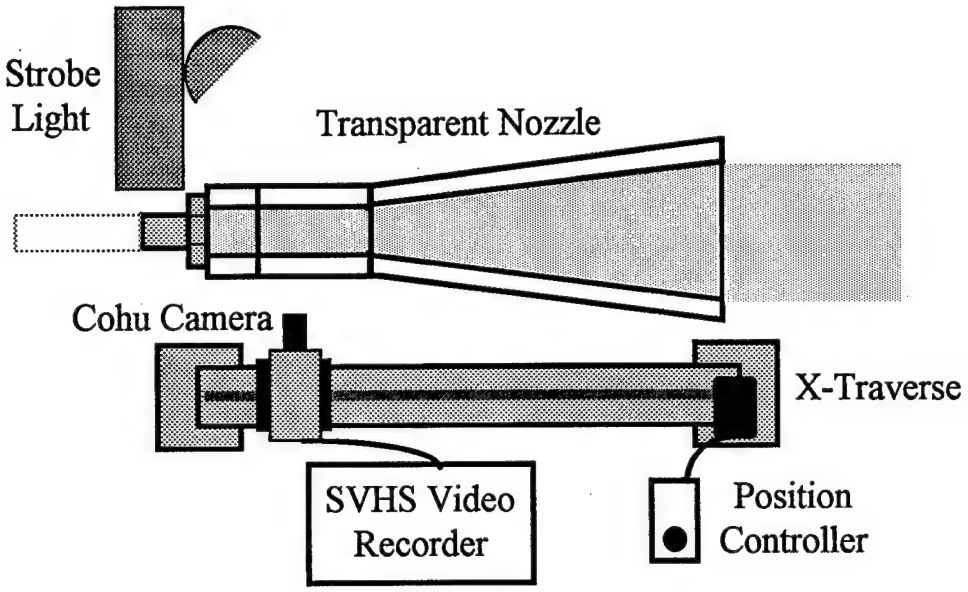

Figure 9 - Imaging Setup

Thirty frames from each location were processed in order to find the variation in particle diameters. Each image undergoes a thresholding process which segments the image into two regions, an object region and a background region. This allows the focus to be on the analysis on the particles. Once the pixels belonging in the specified intensity threshold are identified they are grouped into objects. Two pixels are considered part of the same object if they are horizontally or vertically adjacent. An increased uncertainty occurs with thresholding when the boundaries are not sharply differentiated, as in the case of these images. To overcome the problem of choosing the correct threshold, three different threshold intervals were used on each image and it was determined that any variation in particle size was within our uncertainty. The uncertainty is +/-25

microns for the estimates made inside the nozzle and +/-15 microns outside the nozzle. Unfortunately thresholding only reduces the problem of counting particles that are out of focus as they tend to be less bright. Any particle that is not in the focal distance will appear magnified. Approximately 60% of the particles on each image were out of focus. Forty percent of the particles made it through the thresholding process. Thresholding out the out of focus particles also slightly reduces the size of the in focus particles but all of the in focus particles do make it through the thresholding process.

Another important factor to examine is the particle concentration. Concentration uniformity is important for uniform paint removal. Concentration is estimated along the spanwise direction of the nozzle at the exit by running the same code used to determine the particle size. The transparent nozzle was mounted on a z-traverse and a Cohu CCD camera was focused just downstream of the exit (Figure 10). Thirty images at five spanwise locations were recorded to an SVHS video recorder and the concentration was estimated by counting the particles in these images. The concentration at the exit is given as a volumetric loading of particles per square centimeter.

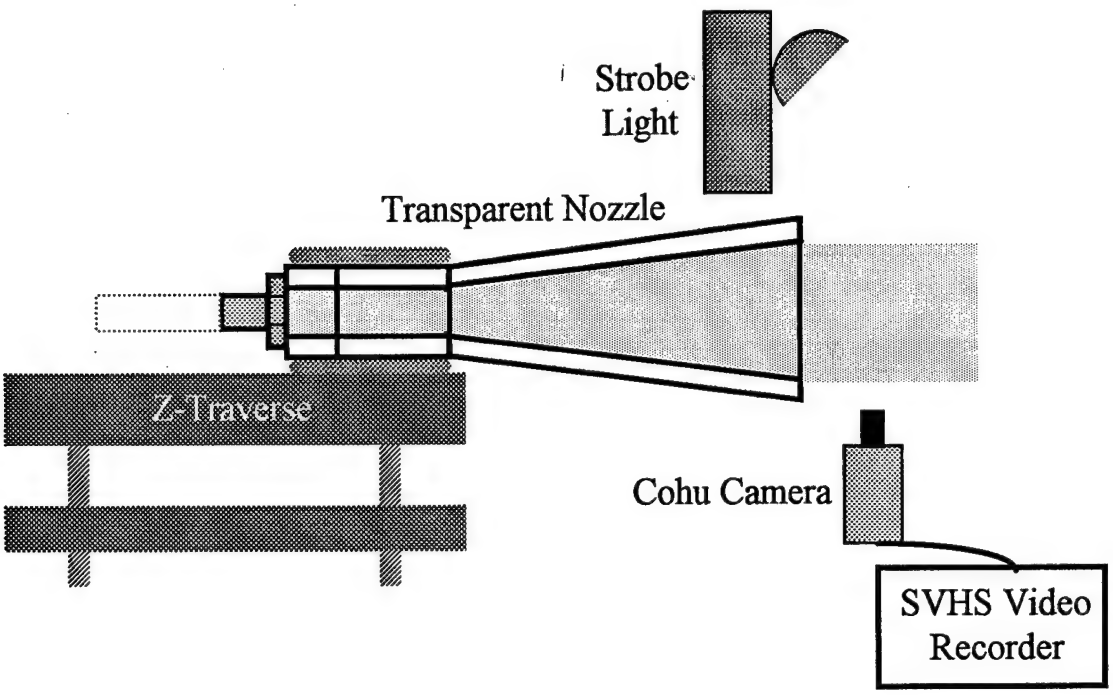

Figure 10 - Exit Concentration Imaging Setup

2.5 FLOW VISUALIZATION

Inside the expansion section of the nozzle, it is impossible to identify individual particles and thus we can only estimate particle concentration by looking at the flow inside this section of the nozzle. A Hi-8 video camcorder was used to recorded images of the flow in the entrance, contraction, and expansion sections of the transparent nozzle. A strobe light was used to freeze the particles. Flow visualization was useful in seeing the concentration in the expansion section and for observing areas of separation and shocks. By also looking at the entrance section, this technique provided verification of particle size and particle break-up in the contraction section.

In conclusion, two test nozzles were constructed in order to examine the flow inside and at the exit of the FLASHJET® nozzle. The metal nozzle mounted with static pressure taps was used to take the static pressure measurements along the centerline of the nozzle and at two

spanwise locations. The transparent Plexiglas nozzle was used to obtain LDA measurements in the entrance section of the nozzle, collect images to be used for estimating particle diameters and particle concentration at the exit, and for visualizing flow patterns in the nozzle. These four anemometry techniques were successful in characterizing the flow and particle behavior throughout the nozzle and at the exit of the nozzle.

3. RESULTS

3.1 NOZZLE SURFACE STATIC PRESSURES

All pressure measurements that will be presented are for a pelletizer pressure of 1100 kPa and a particle loading of 50%. The pressure at the pelletizer can be varied but 1100 kPa is the normal running pressure of the system. Similar results were also found at different pelletizer pressures. Another adjustment that can be made at the pelletizer is the feed rate, or particle

loading. The system is normally run at a feed rate of 50%, but running at a feed rate of 40% showed identical results.

Static pressure measurements were used to map out the pressure distribution in the expansion section of the nozzle. Twenty-one static taps were mounted along the centerline beginning at 2.5 cm downstream of the throat and located every 1.7 cm. Figure 11 shows the static centerline results for the pellets off case. Five runs were taken with only air being sent through the nozzle and these results are plotted along with the average. The data is repeatable to within 3 kPa (10%). In the first half of the nozzle, the drop in static pressure shows that the flow is accelerating through the expansion and then decreases in speed as a result of a shock around x/h=185. Once beyond the shock, the flow then reaccelerates subsonically as it approaches the exit of the nozzle.

The results of the pellets on case is plotted in Figure 12. The six runs are repeatable to within 10 kPa (15%). Adding CO_2 smoothes out the acceleration of the flow before it reaches the shock that decreases the speed of the flow. With the pellet flow off, two small shocks are seen between x/h=100 and x/h=175. These smaller shocks are not present in the CO_2 flow. The addition of CO_2 to the flow also results in the nozzle being run at a higher pressure as well as decreasing the shock and moving it further downstream to x/h=220 (Figure 13). It is not clear whether these changes result simply due to the presence of CO_2 or because addition of CO_2 to the flow increases the mass flow rate through the nozzle. Adding CO_2 to the flow also changes the temperature of the flow which will affectt he pressures. Another difference between running with the pellets off or on is that the velocity of the flow just before the exit of the nozzle is greater when the pellet flow is on.

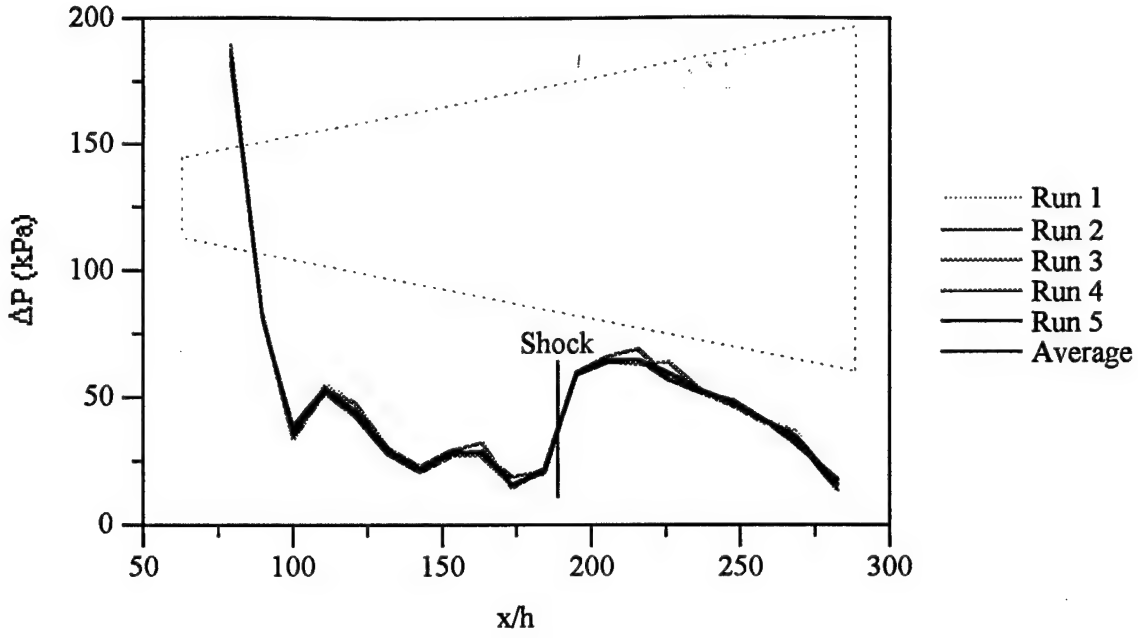

Figure 11 - Centerline Static Pressure Pellet Flow Off

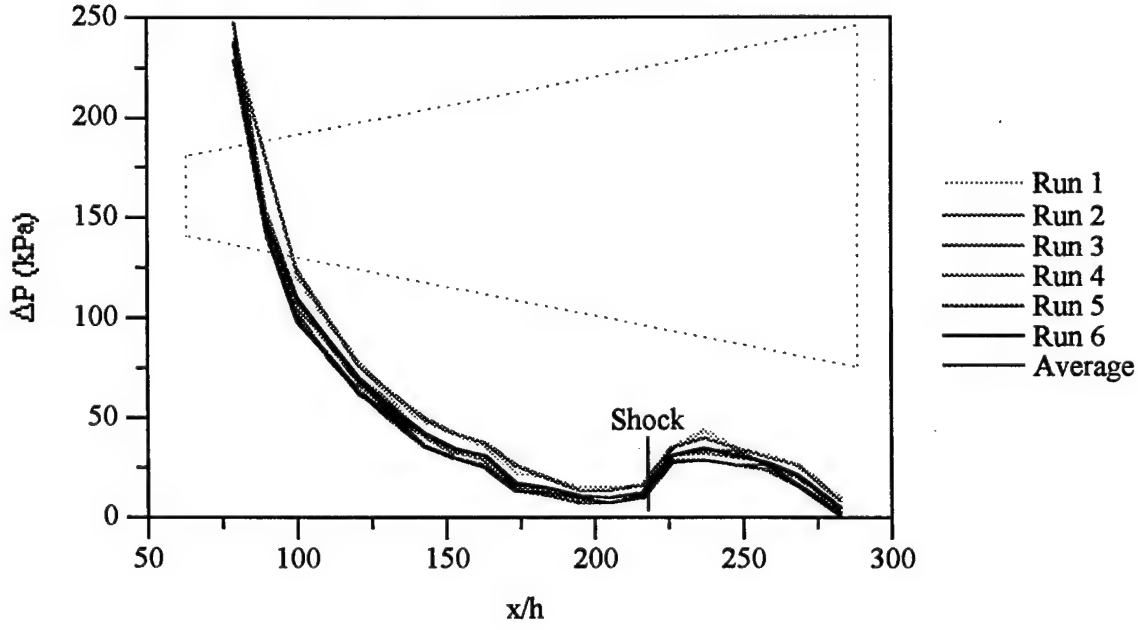

Figure 12 - Centerline Static Pressure Pellet Flow On

Although the pressure at the pelletizer was set at 1100 kPa, there is some fluctuating that takes place because the pelletizer goes through cycles as it is producing pellets and delivering

them to the nozzle. In order to determine how great this fluctation is or if there is some sort of cycle that takes place, pressure readings were taken at the first tap over several minutes. The results are shown in Figure 14. It is easy to see that the pressure does in fact change over the five minute span. The average was found to be 222 kPa and the standard deviation was 3.6 kPa. A large fluctuation corresponded to the automatic cycling of the compressor and was a potential problem during a given run. In order to check the effect of changing pelletizer pressures on static pressure runs, two centerline runs runs were taken relative to the first tap. The results matched the original runs, as seen in Figure 15, which shows the normalized average centerline pressure distribution for all four cases.

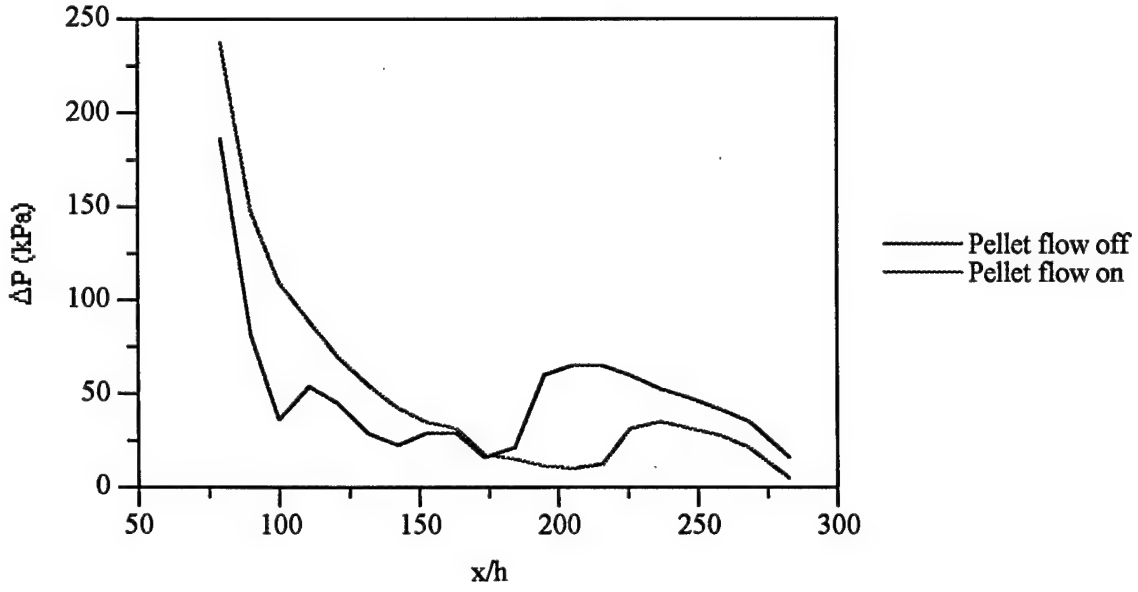

Figure 13 - Average Centerline Static Pressure

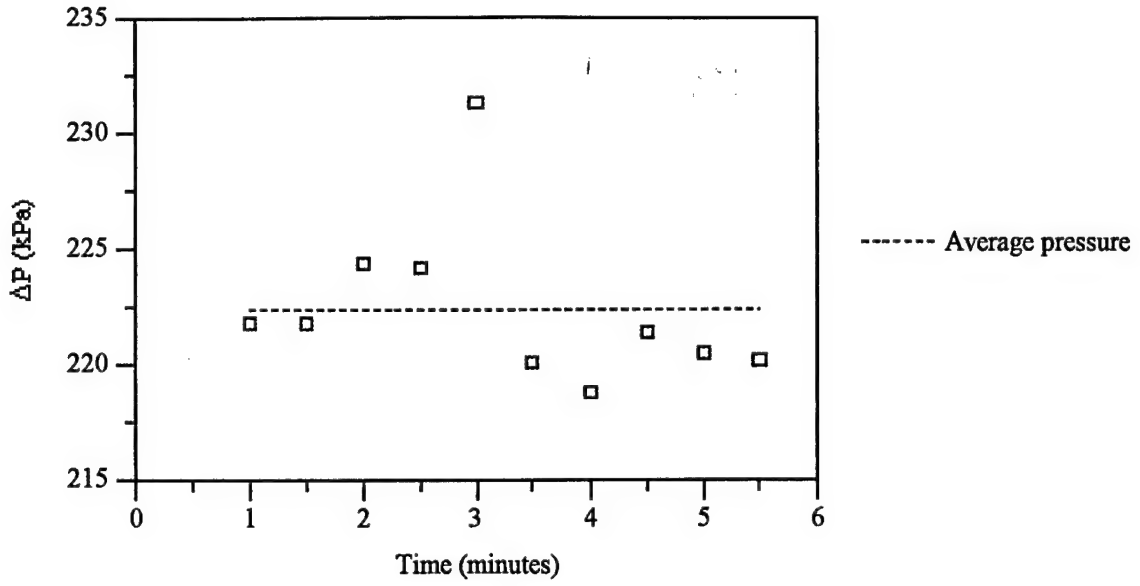

Figure 14 - Static Pressure at Tap 1

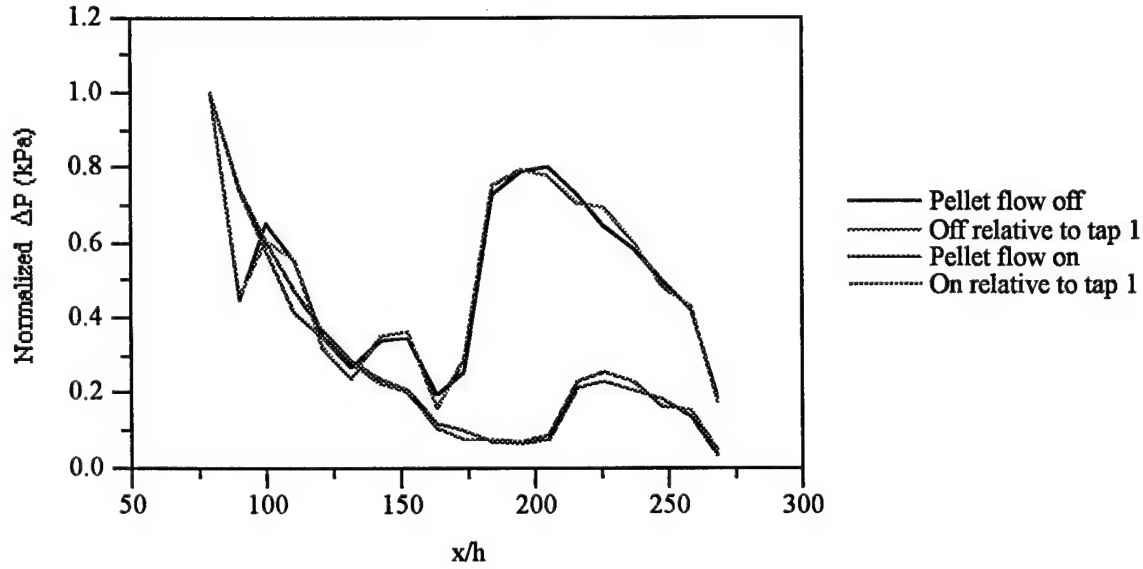

Figure 15 - Normalized Centerline Static Pressure

Static spanwise pressure measurements were taken at x/h=216 and x/h=283. Seven pressure taps are mounted 1.4 cm apart at x/h=216. From the centerline results, the x/h=216 position is located after the shock when the pellet flow is off and before the shock when the pellet

flow is on. Four runs were taken at this location with the pellet flow off and these results are shown in Figure 16. The runs show a repeatability better than 4 kPa (8%). This case appears to show some separation along the edges where the pressure drops slightly. When pellets are introduced into the flow the separation is no longer visible on the right side and the largest deviation between the runs clearly occurs at the center of the nozzle (Figure 17). When the pellet flow is turned on the repeatability of the runs is within 3 kPa (20%). Plotting the average from each case together shows that adding pellets to the flow reduces the pressure at this location (Figure 18). The more uniform separation occurs with the pellets off at this location which for this case is just after the position of the shock.

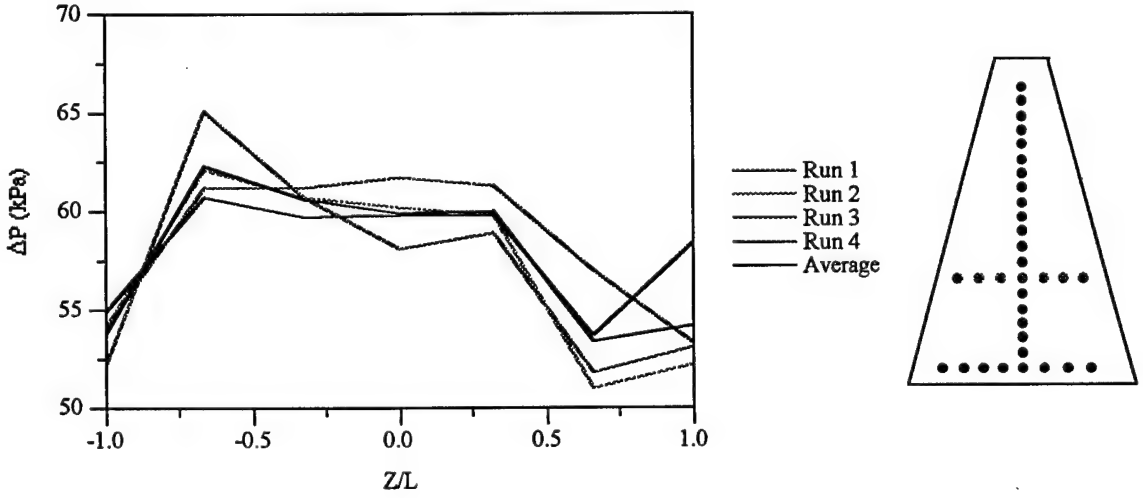

Figure 16 - Spanwise Static Pressure at x/h=216 Pellet Flow Off

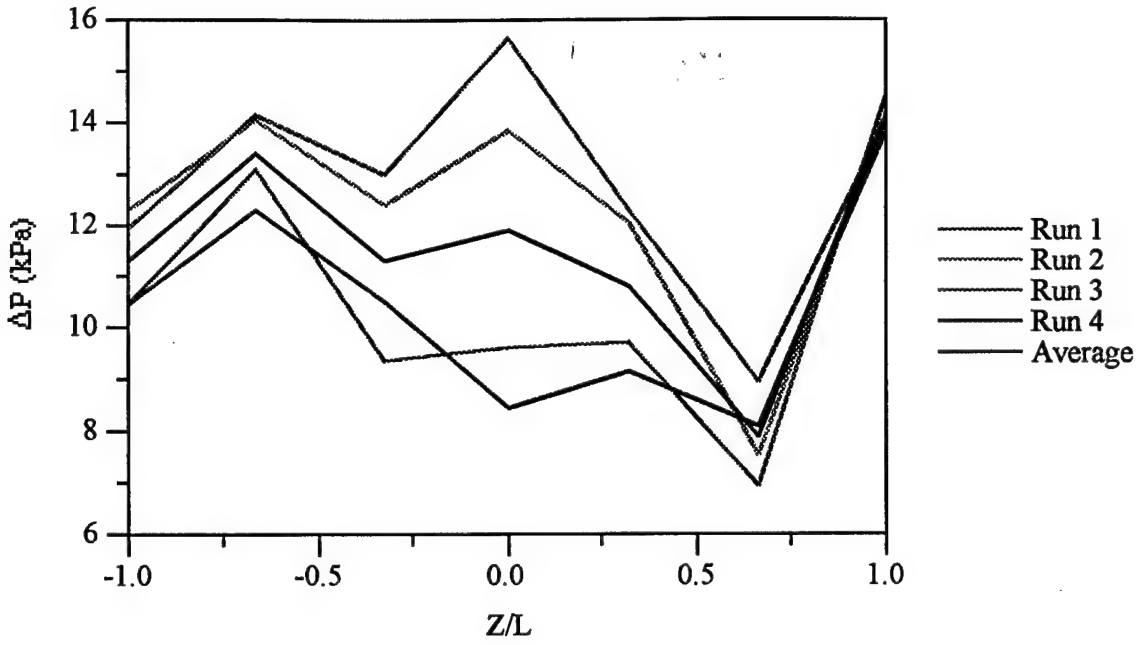

Figure 17 - Spanwise Static Pressure at x/h=216 Pellet Flow On

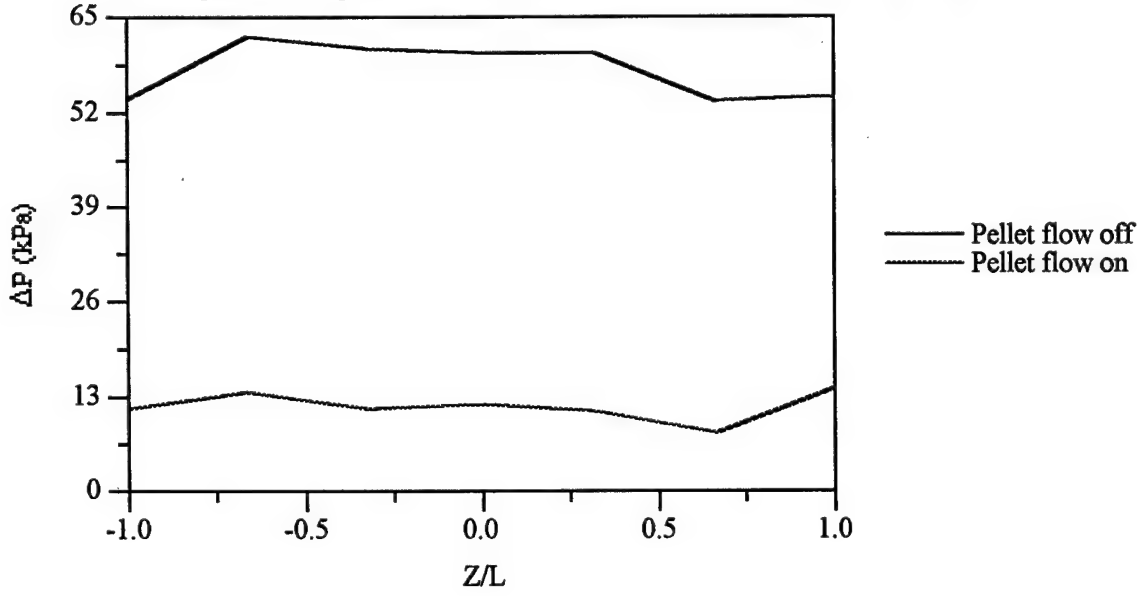

Figure 18 - Average Spanwise Pressure at x/h=216

Eight pressure taps were mounted 1.8 cm apart at x/h=283, just downstream of the shock. This spanwise location is just before the exit of the nozzle (x/h=288). Four runs were taken with and without the CO_2 pellet flow on. The results in Figure 19 and Figure 20 show a separated

region along both edges without and with pellet flow. The repeatability for each case is within 2 kPa (25%) and 4 kPa (30%), respectively. As in the first spanwise location, adding CO_2 drops the pressure across this spanwise location (Figure 21). The separtion is also more prominent in the pellets on case. Comparing the two spanwise locations, with the pellets off, in Figure 22, shows that the pressure drops at x/h=283 as expected due to the flow speeding up as it reaches the exit of the nozzle. The separated region is visible along both edges at x/h=216 but is more prominent along one edge at x/h=283. When the pellet flow is turned on, the same pressure drop occurs at x/h=283 and now the separated region occurs along both edges at x/h=283. Figure 23 also shows that adding CO_2 to the flow also causes an increase in pressure along one edge at both locations but it is greatest at x/h=216.

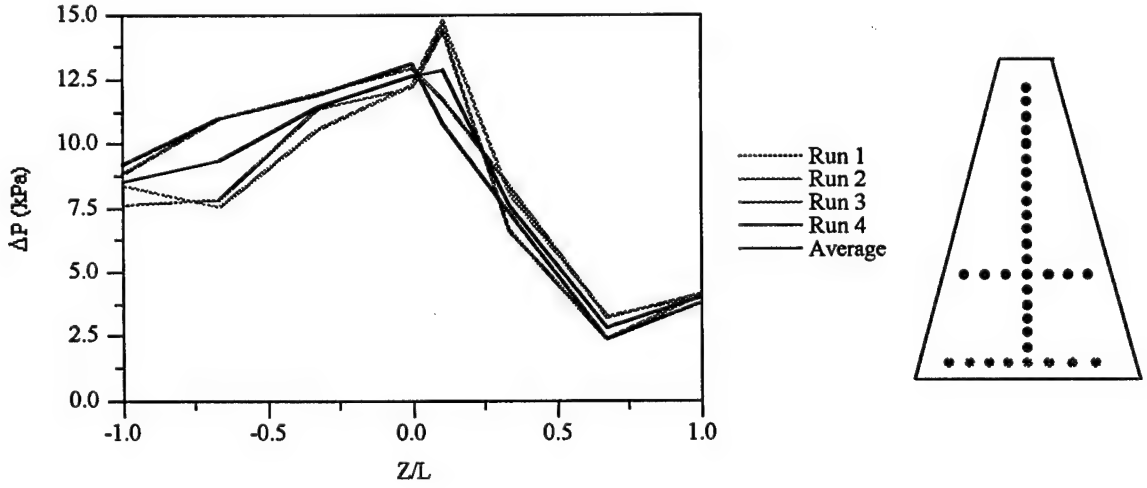

Figure 19 - Spanwise Static Pressure at x/h=283 Pellet Flow Off

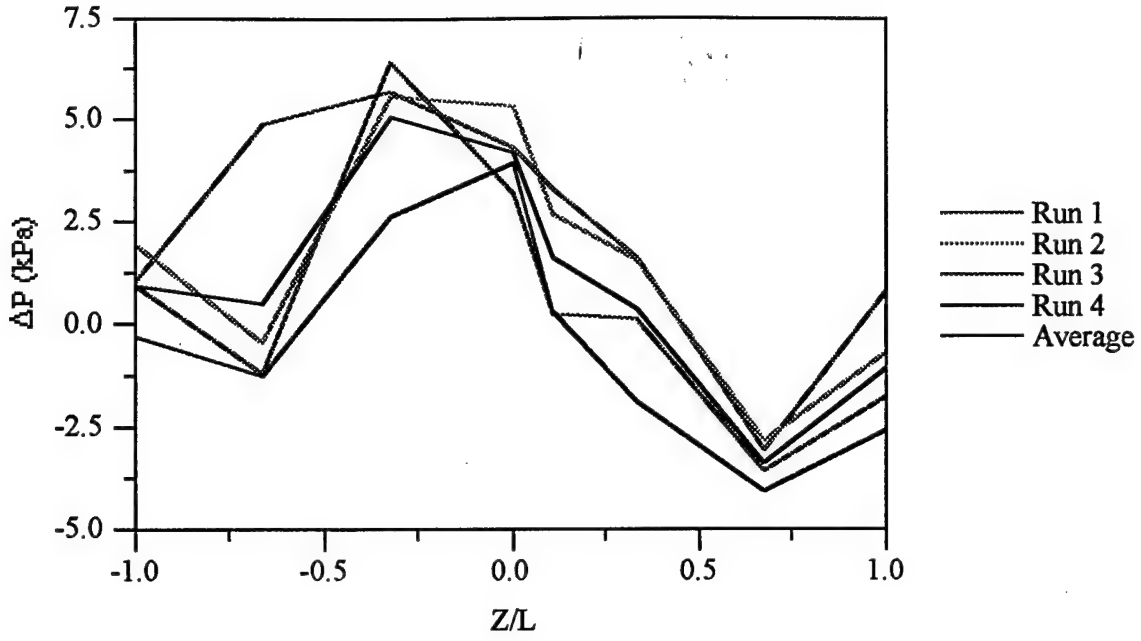

Figure 20 - Spanwise Static Pressure at x/h=283 Pellet Flow On

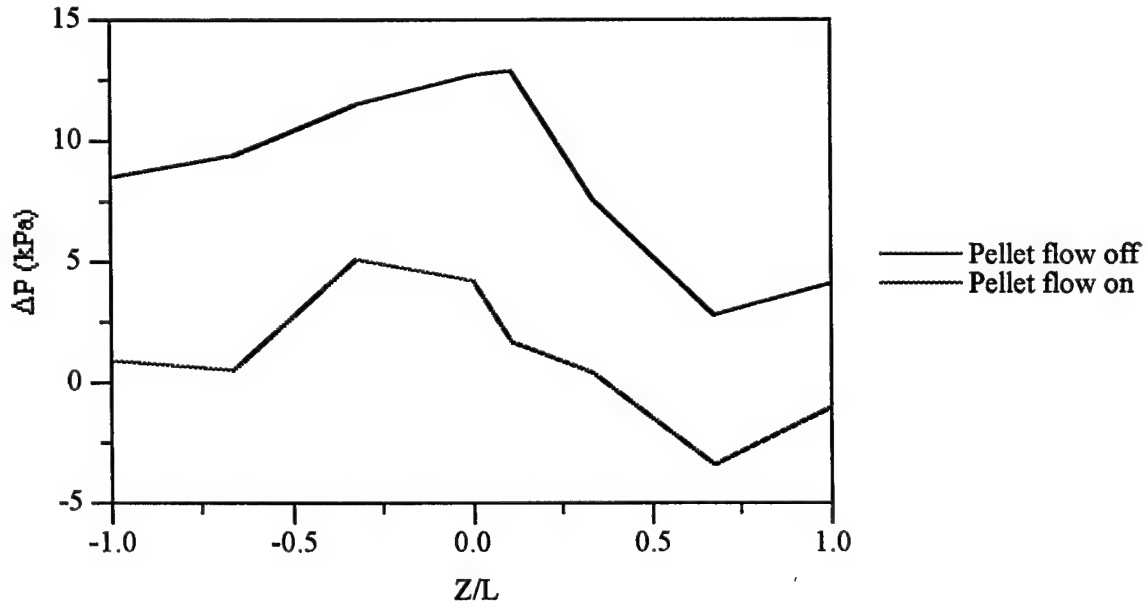

Figure 21 - Average Spanwise Static Pressure at x/h=283

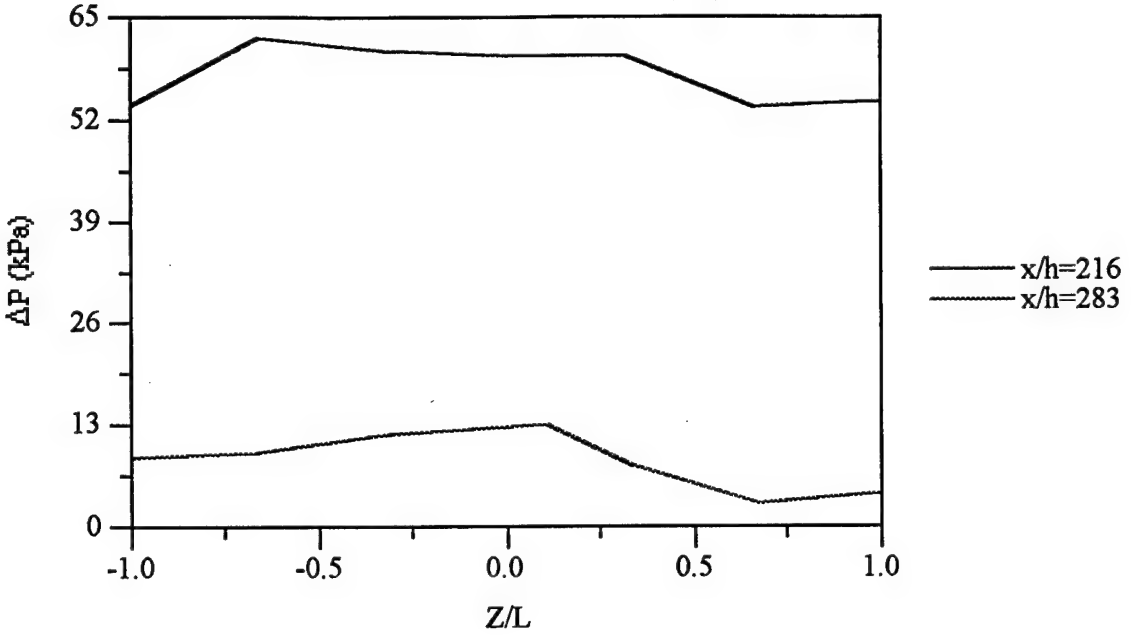

Figure 22 - Average Spanwise Static Pressure Pellet Flow Off

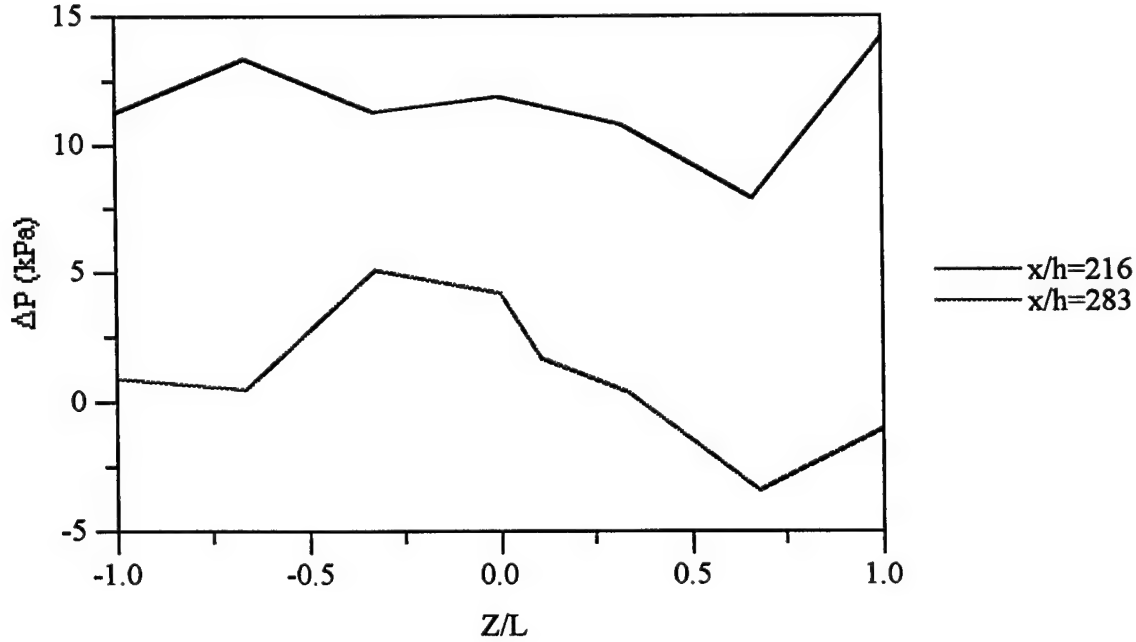

Figure 23 - Average Spanwise Static Pressure Pellet Flow On

The pressure distribution inside the nozzle shows that the flow is accelerating through the expansion section and then decreases in speed as a result of a shock before reaccelerating as it reaches the exit. The location and magnitude of the shock is dependent upon the flow. Adding CO_2 to the flow moves the shock further downstream. Also, with the pellet flow on, the nozzle is run at a higher pressure. The results show that adding particles to the air flow moves the shock downstream and also reduces its strength. A drop in static pressure at the edges of the spanwise locations indicates a separated region at x/h=216 for the case where the pellet flow is off and for both cases at x/h=283. The pressure contours in the expansion section for the pellet flow off and on are shown in Figure 24.

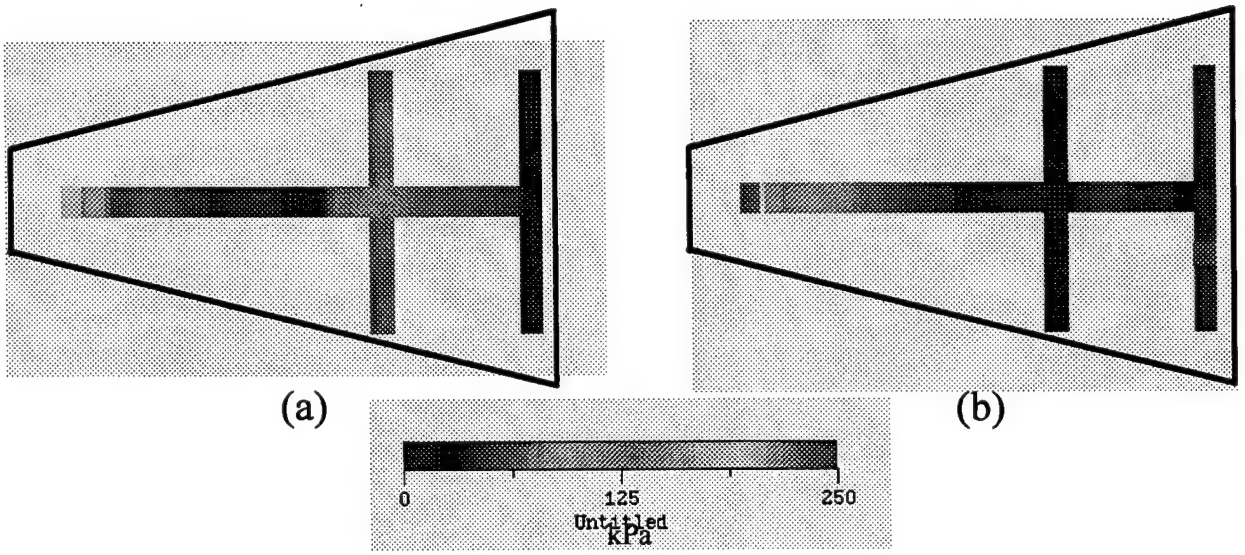

Figure 24 - Pressure Contour Plots (a) Pellet Flow Off, (b) Pellet Flow On

3.2 STAGNATION PRESSURE PROFILES

Stagnation pressure measurements were taken at the exit of the transparent nozzle. Four runs were averaged for the air only case and two runs were averaged for the pellets on case. The centerline results are plotted in Figure 25. Both cases show that the nozzle follows a classic jet decay but the pressures are higher when the particles are introduced into the flow. The static results showed that the pellets on flow had a lower pressure just before the exit. This lower pressure for the pellets on case is also seen in the centerline stagnation results. This indicates a lower exit velocity of the flow when the CO_2 is turned on.

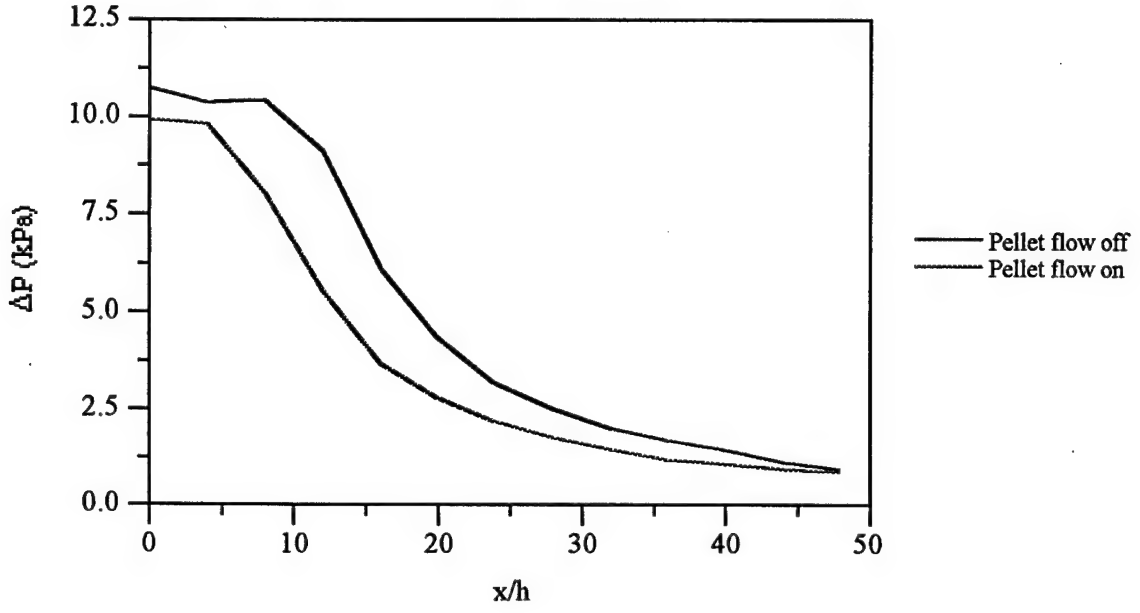

Figure 25 - Centerline Stagnation Pressure

3.3 LDA MEASUREMENTS

LDA measurements were taken in order to obtain initial particle velocities for future numerical simulation work. LDA measurements were taken along the centerline in the entrance of the transparent nozzle. The particles in the entrance section of the nozzle are seen in Figure 26. Figure 27 shows particle velocities in the entrance section and in the beginning of the contraction section. The particles enter the nozzle around 10 m/s. Then there is a slight initial dip due to the area change in going from a round hose to a square nozzle (Figure 28). The third point is located just before the entrance to the contraction section. Finally, the particles begin to accelerate as they enter the contraction at point four. The standard deviation across all measurements is approximately 0.9 m/s. Unfortunately, the LDA setup was incapable of obtaining velocities throughout the length of the nozzle or at the exit. Based on the pressure results and the entrance velocities, it is assumed that the particles continue to get accelerated down the nozzle, most likely crashing into the walls on the way down; breaking up and reducing speed. This provides initial conditions for future numerical simulations.

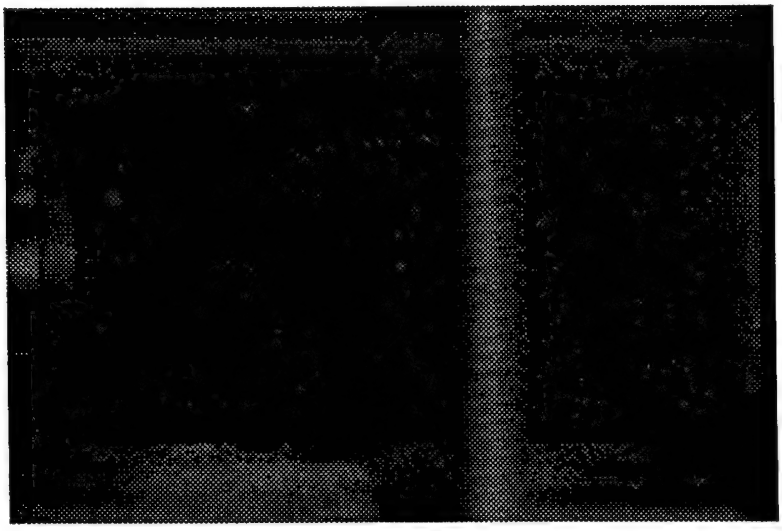

Figure 26 - Particles Entering Nozzle

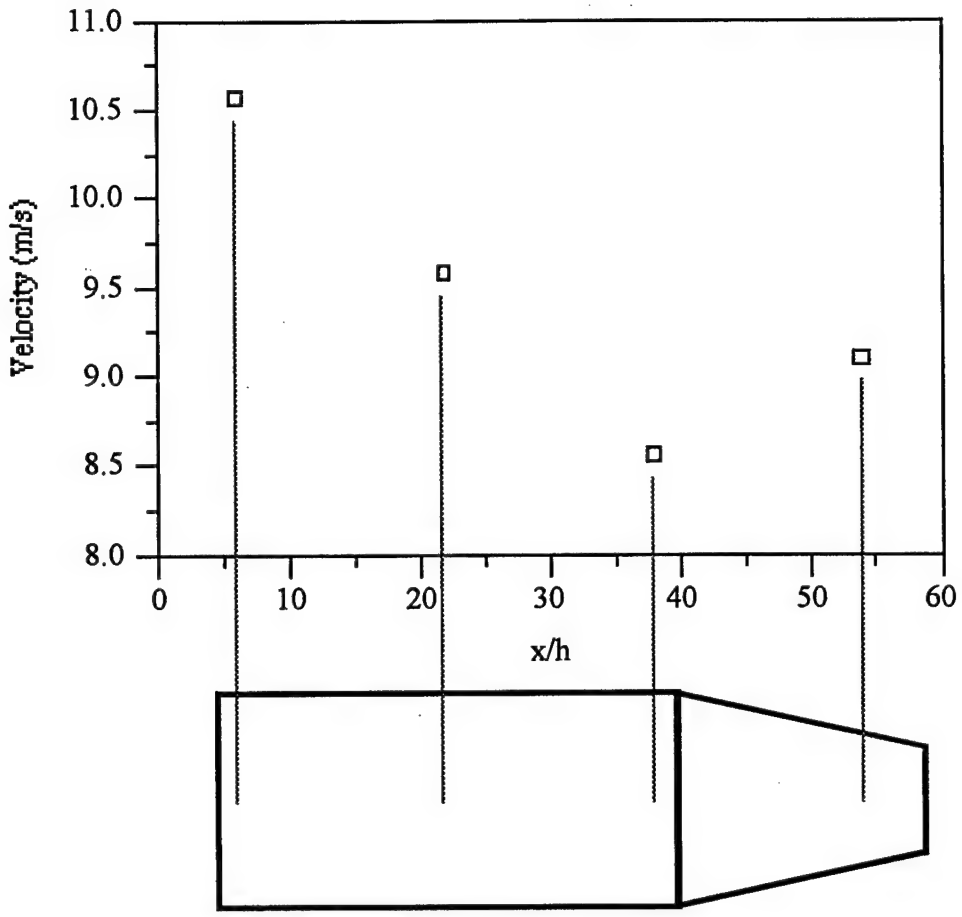

Figure 27 - LDA Velocity Measurements

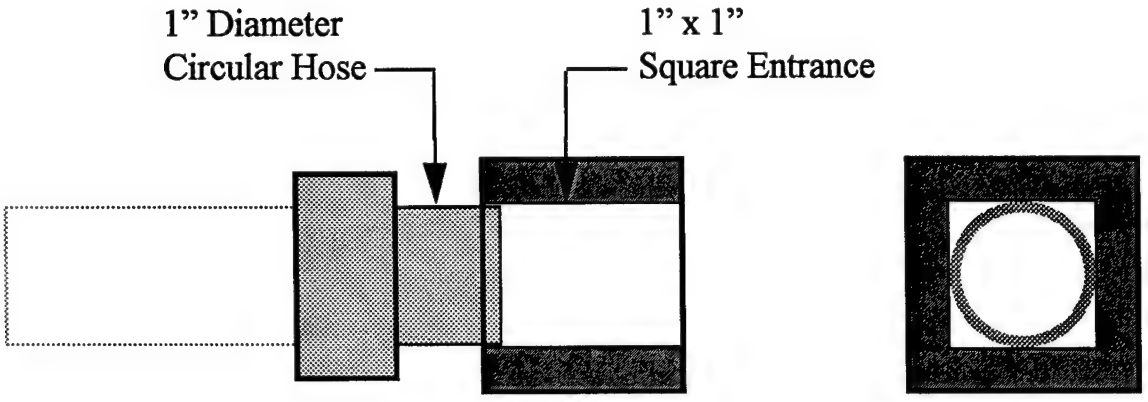

Figure 28 - Entrance Section

3.4 PARTICLE SIZING

In order to see the effects of collisions, particle diameters were estimated from selected images. As one might expect, the particles impinge on the inside walls as they travel through the nozzle (Figure 29). Looking at some sample images taken before the contraction (Figure 30), after the contraction (Figure 31), and at the exit (Figure 32), it is clear that the particles decrease in size as a results of these collisions that take place as the particles are accelerated through the nozzle. The largest particles that are observed exiting the nozzle are approximately one quarter of the size of the largest particles that were detected entering the nozzle from the hose. Out of focus particles are also visible in these non-thresholded images. These particles do not appear true to size and can be distinguished from the in focus particles because they are not as bright and their boundaries are less prominently defined.

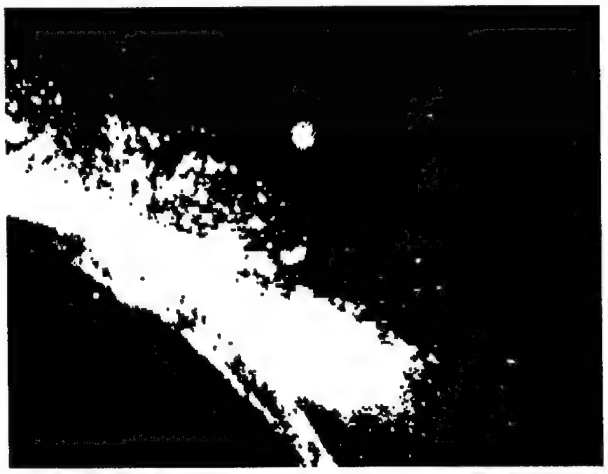

Figure 29 - Particle Collision and Break-Up

One would expect that the average diameter would decrease at each location downstream. The range of particle diameters at the entrance, after the contraction, and after the expansion of the nozzle are shown in Figure 33. The particle size decreases when observing particle diameters just after the contraction and at the exit, but due to a large number of sub 100 micron particles at the entrance, the average size before the contraction is less than what was anticipated. The particle diameter histogram in Figure 34 shows the large number of particles in the first bin of sizes at the first location. Although there are also even smaller particles detected at the second location, the number of these particles is substantially less than the number of slightly larger particles present at the first location. Although the average size is less at the entrance than at the exit, none of the particles that enter the nozzle with diameters greater than 500 micron are observed exiting the nozzle. There are some particles that are exiting the nozzle around 500 micron which would suggest that some particles have minimal contact with the walls and therefore do not undergo the same amount of breakup as the majority of the other particles. Most likely, these larger less frequently exiting particles are important in doing substantial work on the surface. The difference in the range of diameters between the first and second locations is greater than the range of diameters between the second and third locations, which implies that most of the breakup is a result of particle collisions that occur in or near the contraction. Since the maximum diameter at the exit is shown to be less than the maximum diameter after the contraction, this indicates that collisions are taking place in the expansion section but that these collisions occur less often and have a less dramatic effect on particle breakup.

By looking at the diameter results and removing all the particles with diameters less than 50 microns at each location, the histogram (Figure 35) and average particle diameter (Figure 36) changes. The first obvious difference is that the minimum diameter increases, but more

importantly the average diameter also increases. These new results now show that the average diameter is greatest at the entrance of the nozzle and decreases at each location downstream. Although the number of the smallest particles is still greatest at the entrance, there are also more of the intermediate size particles at this location. Another factor which raises the entrance section average is the presence of the larger particles at this location that are not seen at the other locations.

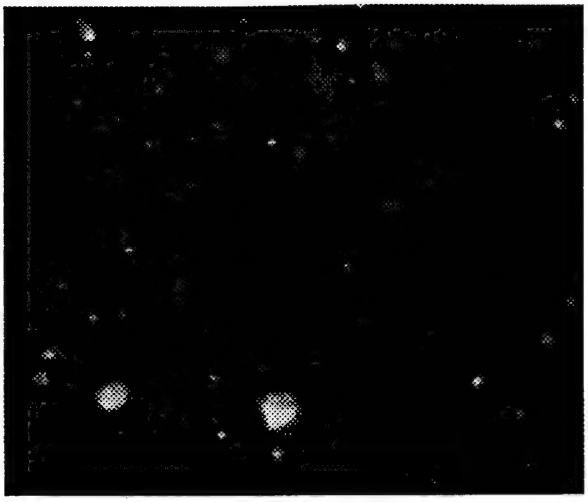

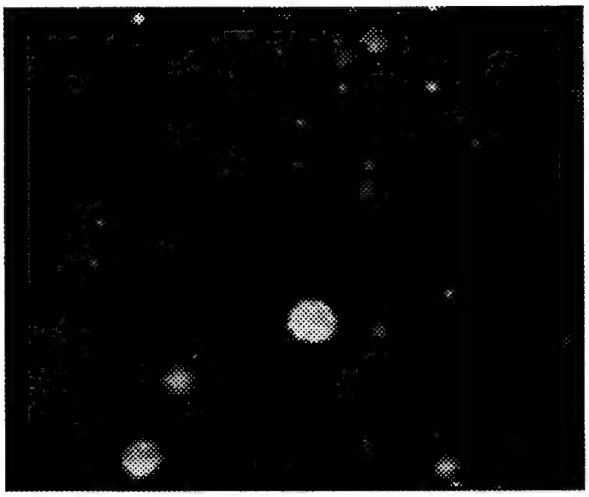

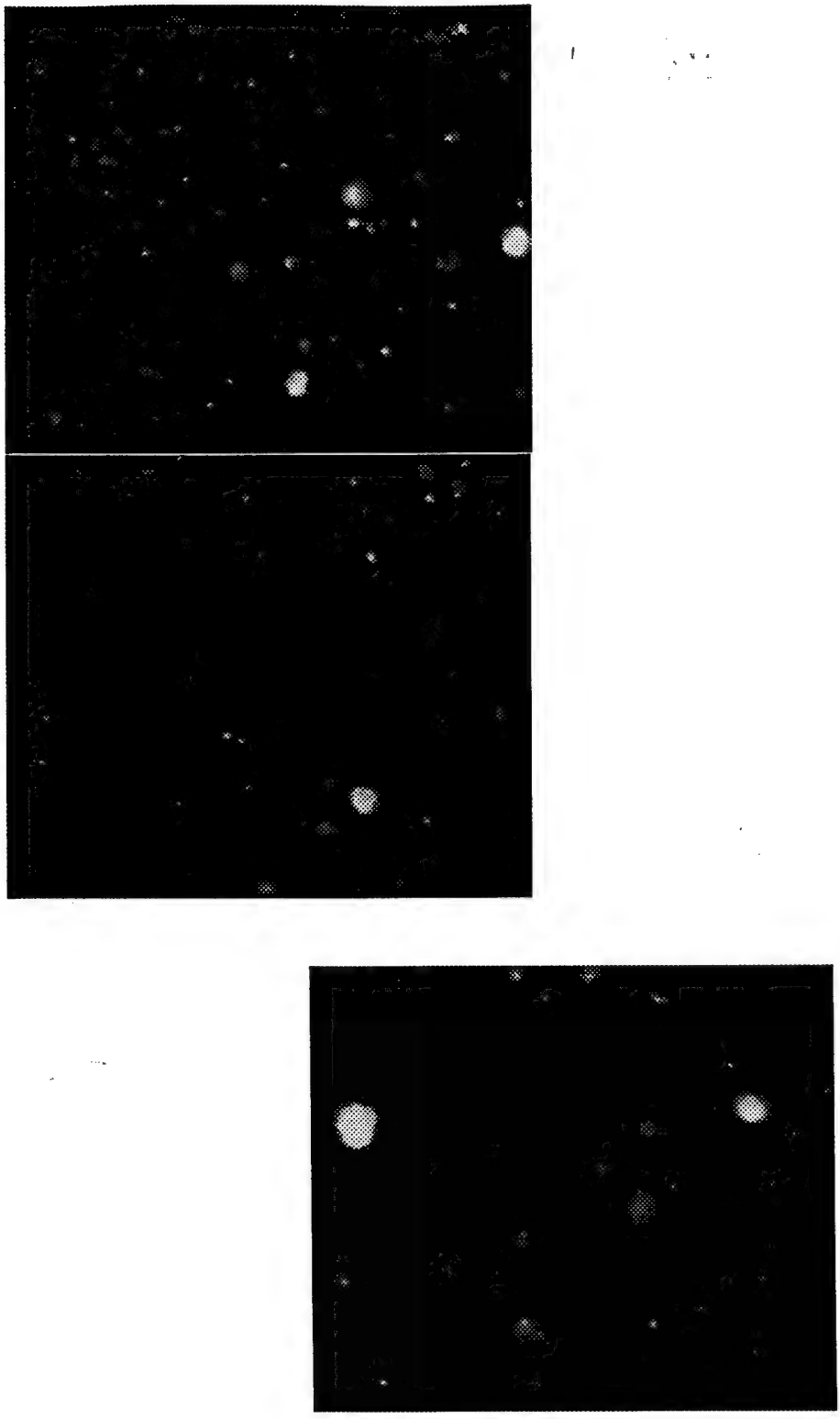

Figure 30 - Sample Images Before Contraction

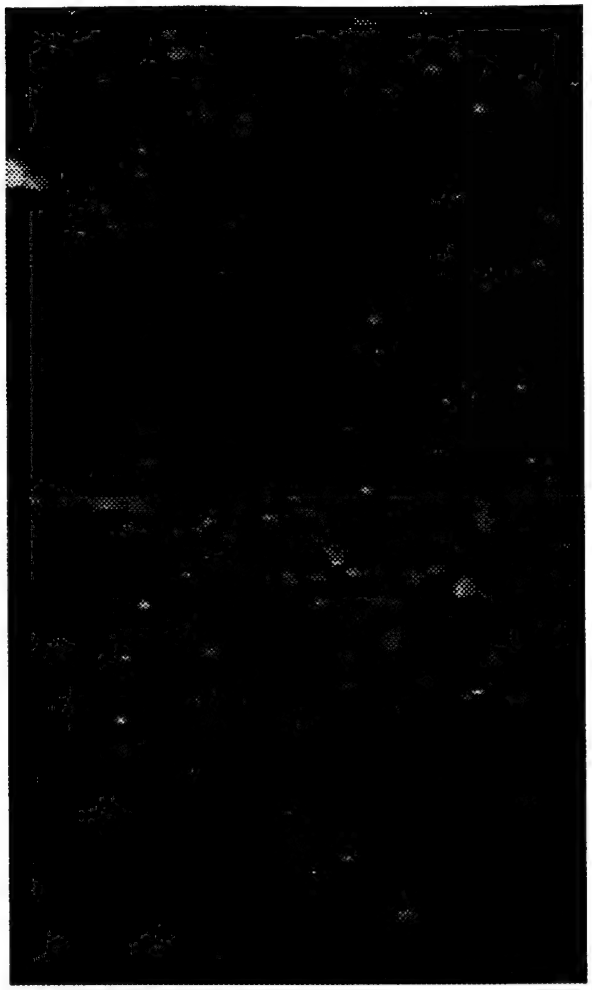

Figure 31 - Sample Images After Contraction

Figure 32 - Sample Images Exit

Although there is a great amount of uncertainty associated with this technique much of it has been overcome through a type of filtering process. The large number of out of focus particles in each image has been eliminated by thresholding the images. This thresholding process may decrease the particle size slightly but it does not remove any of the in focus particles from the image. Any noise that may be present on the images would also skew the results but it is assumed that all noise is filtered out when the images are thresholded. On each image one pixel is equal to 25 microns so that all the estimated diameters are plus or minus 25 microns.

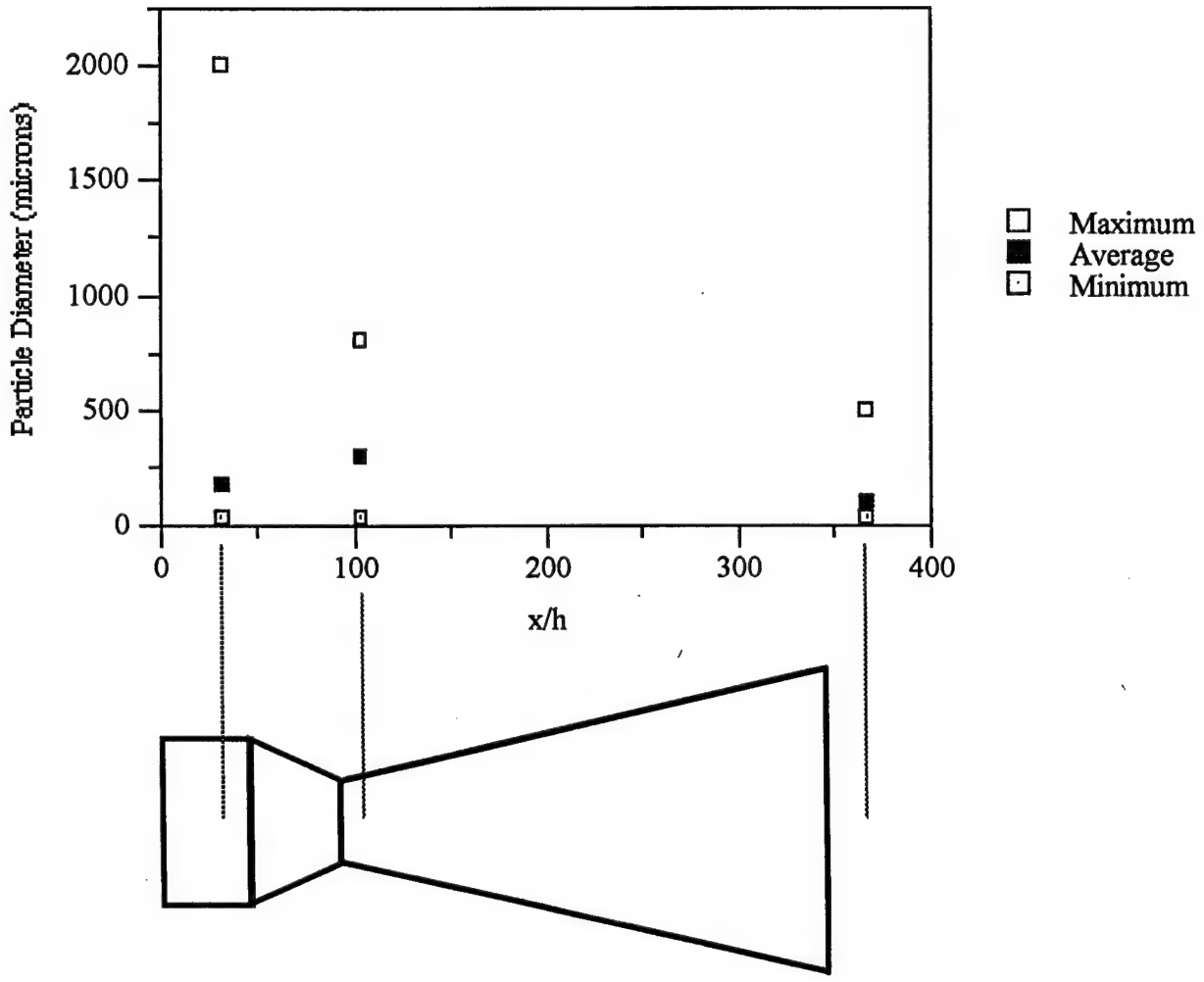

Figure 33 - Range of Particle Diameters

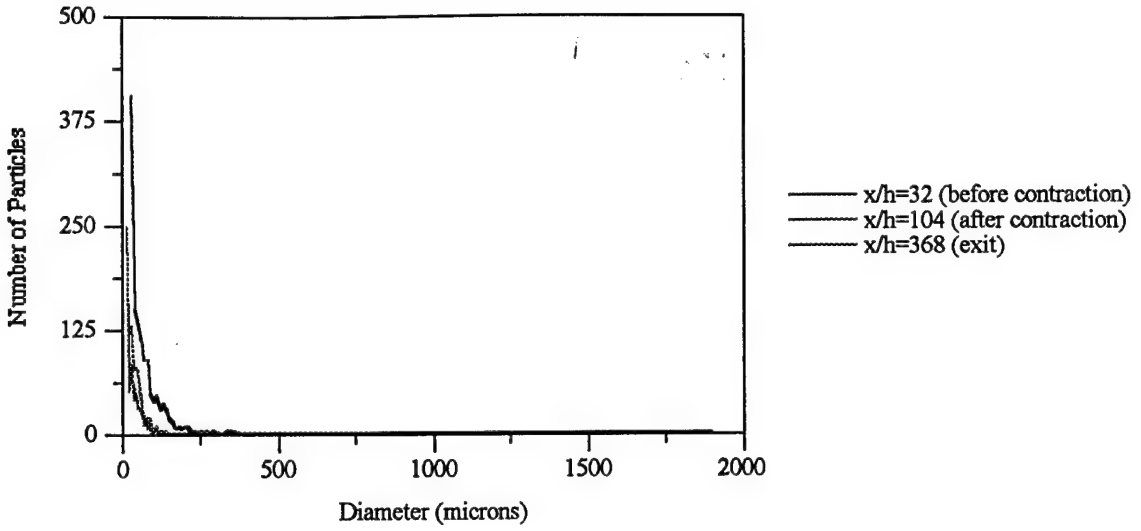

Figure 34 - Particle Diameter Histogram

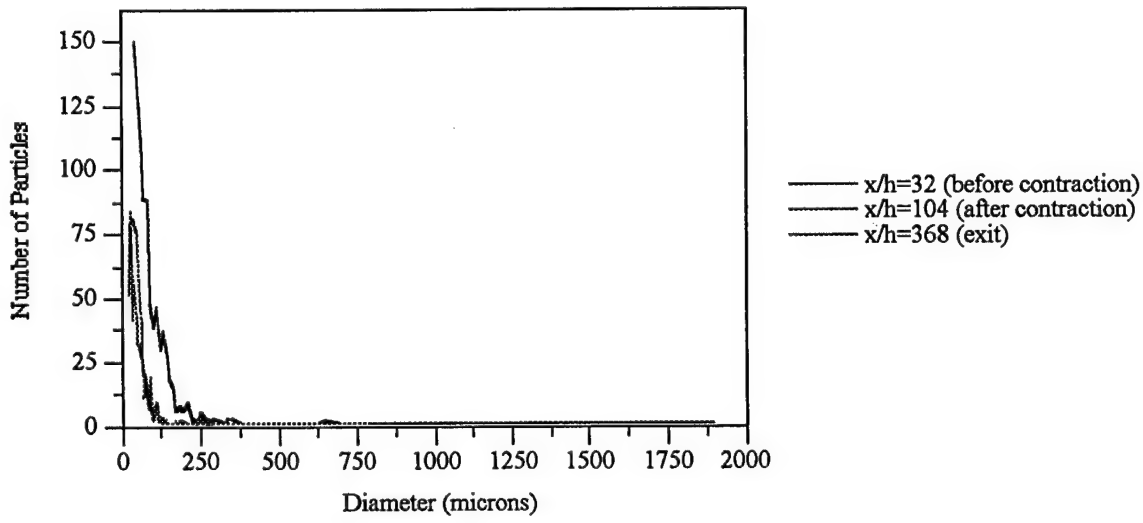

Figure 35 - Particle Diameter Histogram for Particles Greater than 50 microns

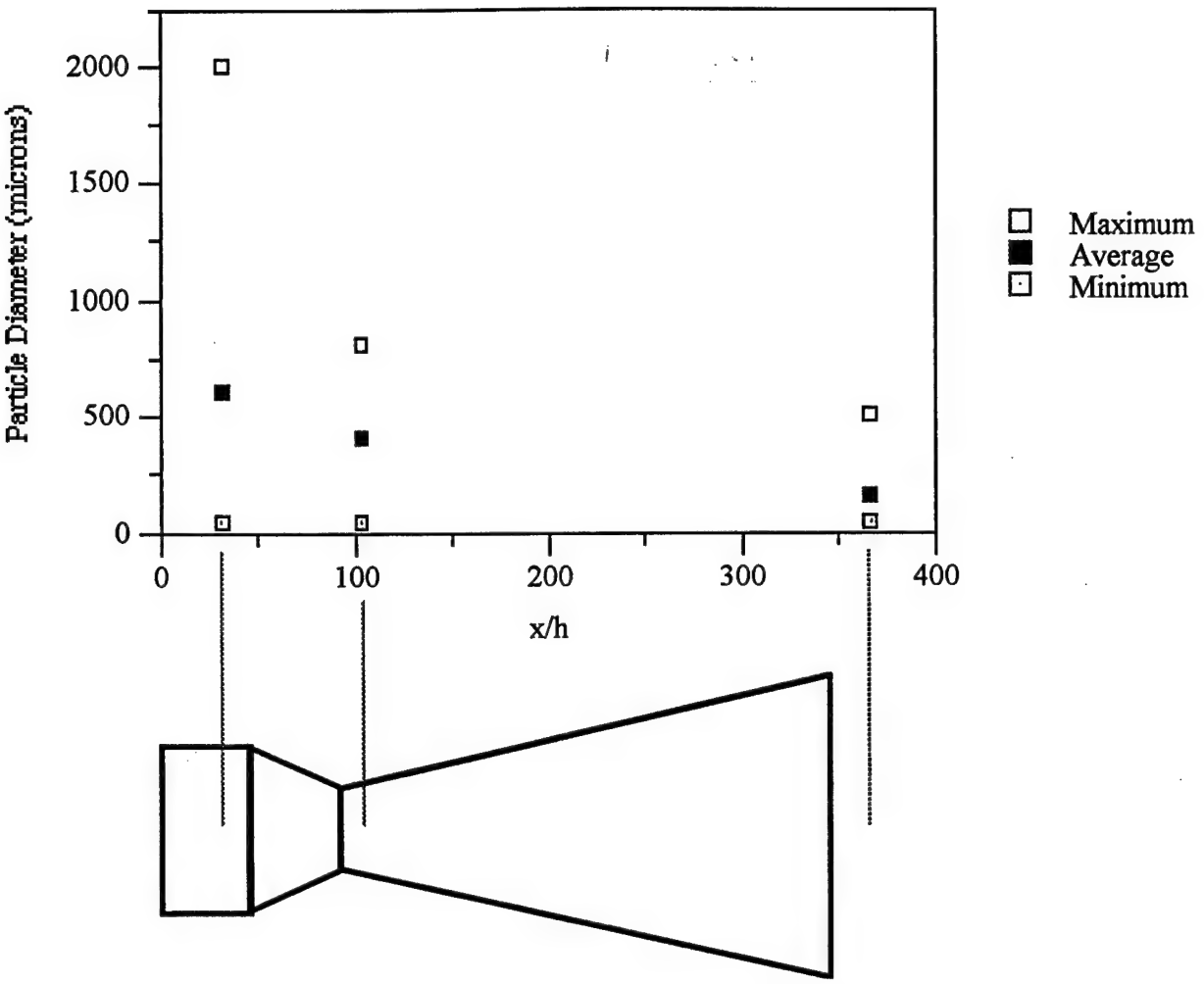

Figure 36 - Range of Particle Diameters Greater than 50 microns

Learning more about the particle sizes throughout the nozzle leads to confirmation of the assumption that the particles get broken up as they travel through the nozzle. The particles enter the nozzle with an average diameter of 600 microns, exit the contraction at 400 microns and finally exit the expansion at 150 microns. It appears that most of the collisions and subsequent breaking up of the particles occur in the contraction due to the large decrease in the maximum diameters found between the entrance and after the contraction. The largest particles entering the

nozzle are around 2000 microns and the largest particles exiting the contraction are around 800 microns.

3.5 PARTICLE CONCENTRATION

The concentration of particles at the exit of the transparent nozzle was estimated by determining the particle loading. Counting particles in the images at the five areas along the exit (Figure 37) shows an average of 83 particles per image (standard deviation of 16 particles). This corresponds to an average particle loading of about 4 particles per square centimeter. The standard deviation across all measurements is approximately 0.8 particles per square centimeter. Figure 38 shows that the concentration is neither uniform nor symmetric across the exit and the maximum loading occurs at the center of the nozzle. The concentration decreases in the separated regions along the edge of the nozzle. The points that are plotted are located at the center of the imaging areas.

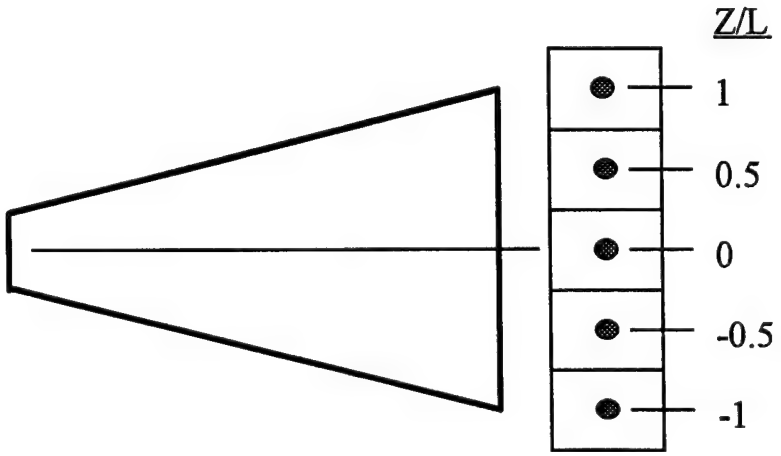

Figure 37 - Spanwise Areas

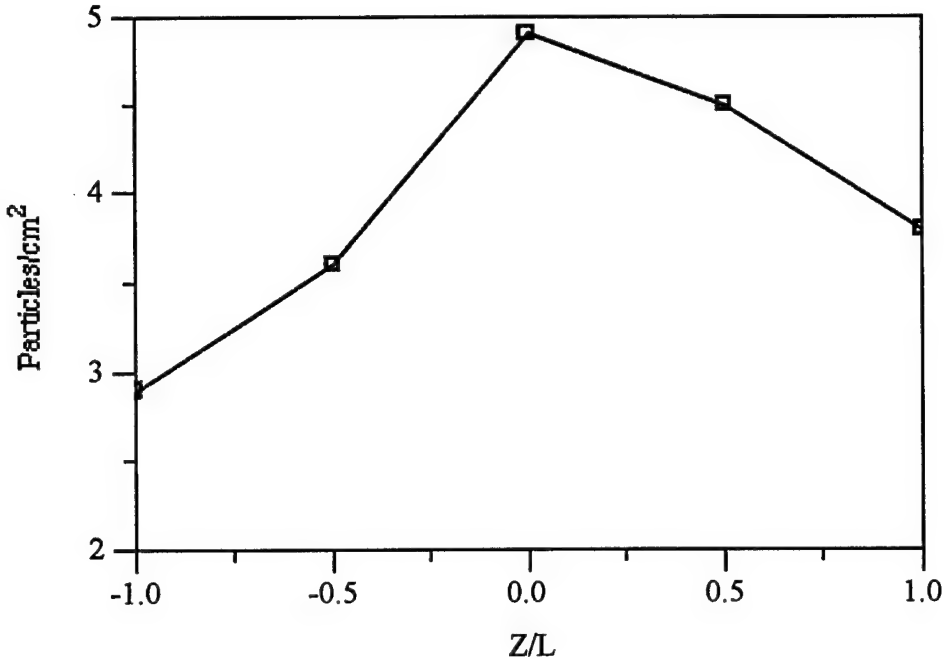

Figure 38 - Particle Concentration Outside Transparent Nozzle at x/h=32

3.6 FLOW VISUALIZATION

Inside the expansion section it is very difficult to identify individual particles. Therefore, flow visualization was used to get some information on the concentration inside the transparent nozzle. This proved to be an excellent tool in getting a better grasp on what is happening to the flow inside the nozzle. An image of the expansion section is seen in Figure 39. This image shows a uniform concentration at the entrance and an increase in concentration in the lower half as the distance downstream increases. Symmetric separated regions are visible along the top and bottom walls at the exit. An oblique shock can also be seen just beyond the point of separation.

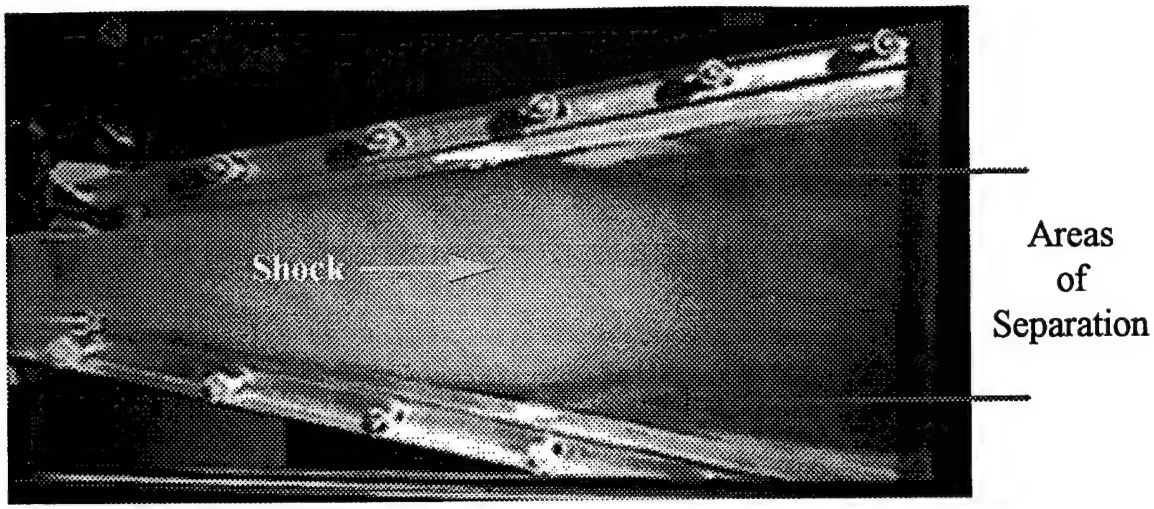

Figure 39 - Expansion Section

There are some images of the expansion section in which individual particle are visible. Although there are not enough particles to to estimate a particle loading, the particle diameters can be estimated and used to verify the particle size results. Only very large particles were visible and the maximum diameter at this location was found to be around 500 microns. Since the flow visualization was able to confirm particle size in the expansion section, flow visualization images from the entrance section were examined to check the diameter results for this part of the nozzle. In the entrance section, particles diameters ranged from around 1500 microns to 500 microns. The smallest particles that can be measured have diamters of around 500 micron, which was the size of the largest particles further downstream in the nozzle. This helps to reaffirm that the particles are in fact breaking up as they travel through the nozzle.

4. DISCUSSION

The interests of this research are on high aspect ratio, high velocity jets and their application to paint stripping techniques. This work specifically looks at the two phase flow inside the high aspect ratio nozzle of an existing paint stripping system developed at McDonnell Douglas Corporation. The main goal was to characterize the flow in the existing setup. Figure 41 shows a schematicof the flow behavior and all the results. Particles enter the nozzle around 10 m/s with diameters as large as 2000 micron. Then as the particles get accelerated through the contraction, they crash into the walls and get broken up, as well as lose speed. Once through the contraction they are again accelerated through the expansion section, where some minor collisions occur, causing more breakup of the particles. Finally, the particles exit the nozzle at an average velocity of 65 m/s, compared to the fluid velocity of about 235 m/s[6], with the largest diameter being around 500 microns.

Focusing on the flow in the expansion section, the flow visualization shows an oblique shock which forms just before the start of the separated region. This observation brings up the question of whether the shock causes the separation or the separation causes the shock. The shock was not visible when only air was traveling through the nozzle but was seen in the centerline static pressure measurements. In fact, the pressure results indicate that introducing the CO_2 particles into the flow runs the nozzle at a higher pressure, decreases the magnitude of the shock and moves its location further downstream. Static pressure measurements at the first spanwise location at x/h=216 more clearly show separation for the air only case but at the second spanwise location at x/h=283 separation is clearly shown along both edges when the pellet flow is boht off and on. These results show that adding CO_2 moves the separated region downstream.

The pressure measurements confirm that the shock and separation are related, as both are moved downstream in the pellets on case.

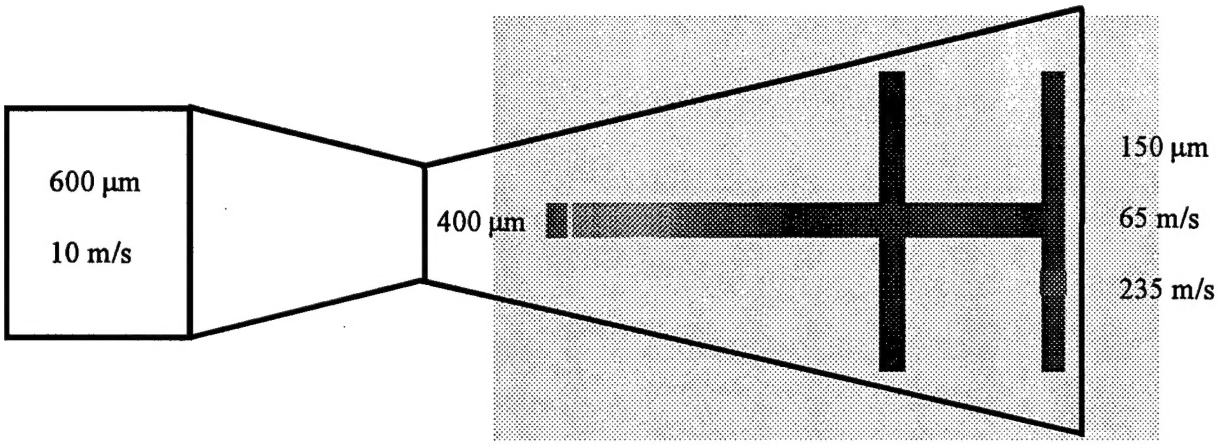

Figure 40 - Flow Behavior

Moving beyond the exit of the nozzle turns the focus to how the particles do their job of removing paint. Although the particle concentration at the exit was not found to be uniform, the nozzle has been proven effective at stripping paint uniformly. The maximum particle loading occurs at the center of the nozzle and the minimum loading appears to be along the edges in the separated region. Since the areas of the flow with less concentration are just as effective at stripping paint as the area of greater concentration, this leads to the conclusion that decreasing the concentration of particles in the center of the flow would not compromise the nozzle's effectiveness in uniformly stripping paint. Another factor to consider is the velocities of the particles. Pothier *et al.*[6] used streak measurements to determine that the average velocity at the exit is 65 m/s. There was a large range of particle velocities due to the varying size particles that are exit the nozzle. The centerline stagnation pressure measurements show that the nozzle follows a classic jet decay both with and without the CO_2 in the flow. Since the particles exit the nozzle at different sizes with varying velocities, and therefore different momentum, it is not clear

how their velocities decay. Pressures were found to be more uniform across the nozzle with the air only flow. Adding CO_2 causes a large pressure difference between the center and the edges which is caused by the separated region. This implies that the velocities are higher in the center of the nozzle but as in the cases of decreased concentration at the edges, the lower edge velocities do not deter from the effectiveness of the nozzle's paint stripping ability. It would seem that the particles exiting the center of the nozzle do not have to be moving with such high velocities to do their job since the slower moving particles that exit at the edges successfully remove paint. Along with the particle loading and velocities, the other important component to consider is size. The particles that exit the nozzle range in diameters from 40 to 500 microns with the average size being 150 microns. It is believed that it is the larger particles that do most of the work on the surface. This assumption came from testing another nozzle from which the particles exitted with higher velocities but smaller diameters and were not able to remove all the waste from the surface.

5. CONCLUSIONS AND FUTURE RESEARCH

This is a study of two phase flow through a high aspect ratio nozzle complicated by the addition of particles. For the first time the particle behavior inside the nozzle was examined and this has lead to several findings. The particles enter the nozzle with diameters ranging from 40 to 2000 micron with an average of 600 micron. The are initially moving around 10 m/s. Moving through the contraction causes breakup of the particles. Addition breakup occurs with some particles as they travel through the expansion. The presence of these CO_2 particles runs the nozzle at a higher pressure and also has an effect on a shock by decreasing its magnitude and moving it further downstream by changing the mass flow rate.

Outside the nozzle the particles range in diameter from 40 to 500 microns with an average of 150 microns. The particle loading was found to be nonuniform and at its greatest at the center of the nozzle. The average particle velocity was estimated to be around 65 m/s[6] which is considerably slower that the fluid velocity whcih is moving around 235 m/s. These three factors need to be considered in order to acheive the goals of reducing the amount of CO_2 that is used, minimize the pressure that is needed to run the system, and come up with design for a more compact nozzle. Optimizing the nozzle will reduce the system's operating costs. Determining the minimum particle velocity and concentration that is necessary to successfully strip paint will reduce the amount of energy that is needed to run the system and reduce the amount of CO_2 that used. The greatest expense of running a working system comes from the cost of the liquid CO_2 so that reducing the the amount of CO_2 that is used could save substantial costs.

There are still a number of unanswered questions associated with this project. One important question is what role the particles play in the heat transfer. Future work will involve numerical simulations and heat transfer studies, and considering all the results to design a more compact nozzle. The velocity results obtained from the LDA measurements will be used as the initial particle velocity inside the nozzle when running numerical simulations. Simulations will be used to confirm the pressure distributions and estimate exit velocities of the flow and particles. Heat transfer studies will be conducted to gain a better understanding of what is happening to the particles as they hit the surface. Finally, after looking at all the results a new, more compact nozzle will be designed.